

Near-threshold Production and Energy-Dependent Electromagnetic Form Factors of Λ_c^+

王维平 (On behalf of BESIII Collaboration)

Johannes Gutenberg University Mainz (JGU)
University of Science and Technology of China (USTC)

第七十五届强子物理在线论坛 (HAPOF)

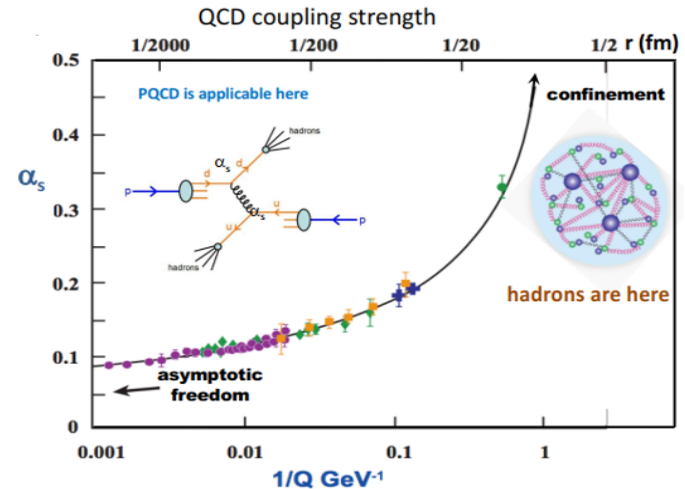
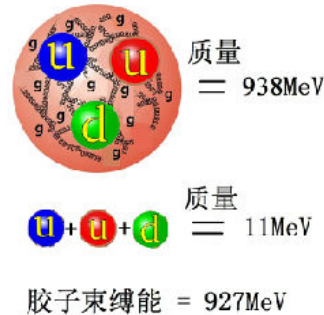
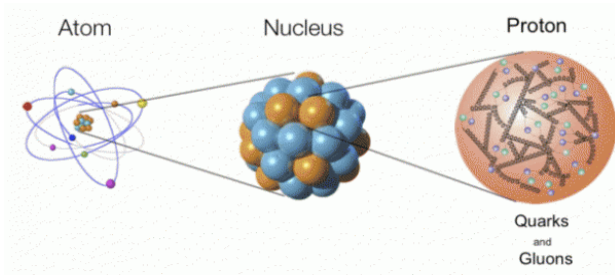
2023年8月4日



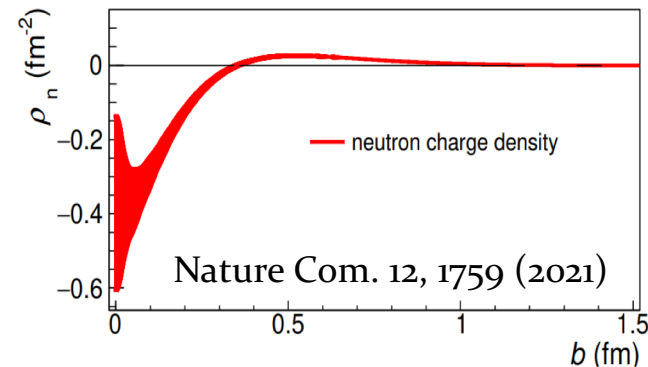
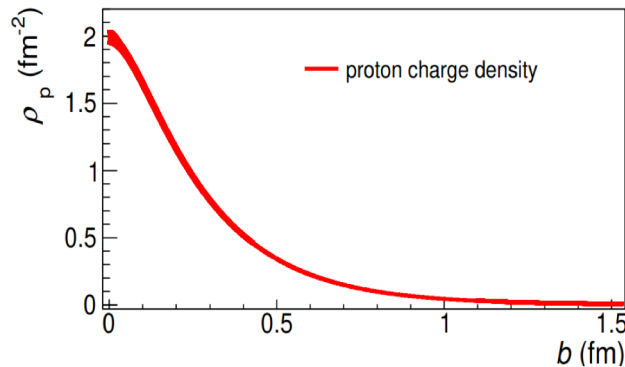
Electromagnetic form factors (EMFFs)

- Nucleons are composite objects with inner structure. At low Q , perturbative QCD does not work well (expansion of coupling constant α_s)

⇒ Nucleon structure must be measured in experiments!



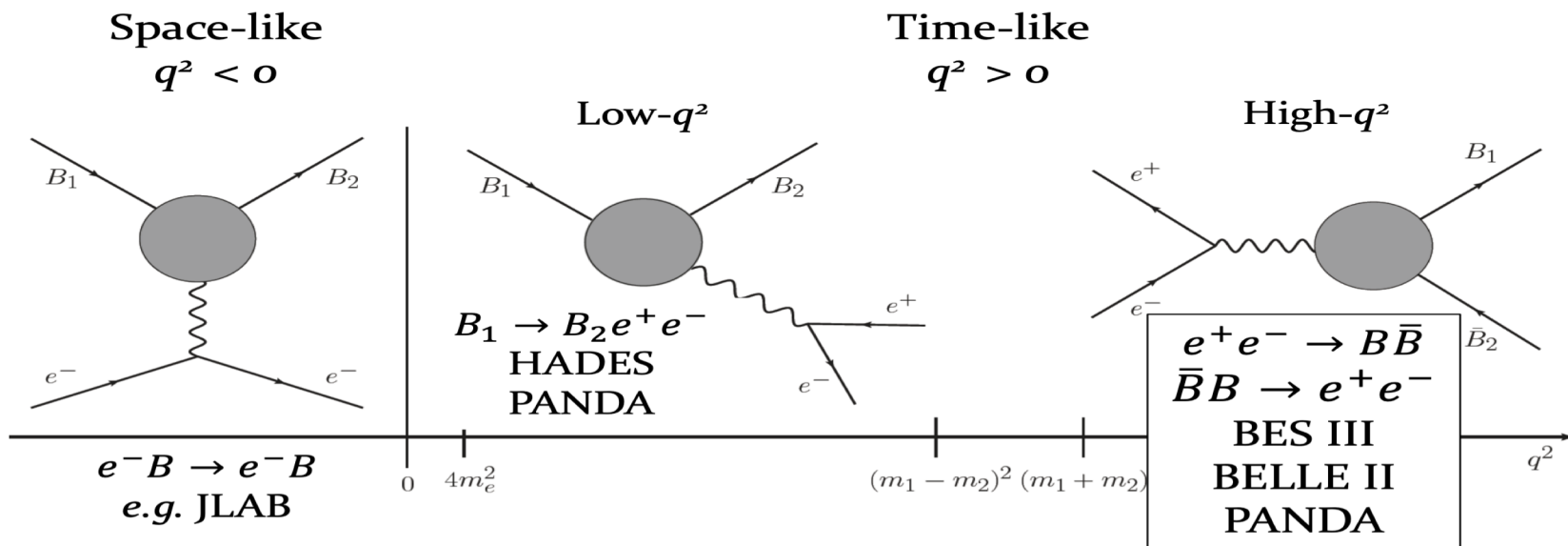
- Using **photon** as a probe, the coupling to nucleon can be expressed in terms EMFFs



Electromagnetic form factors

□ Fundamental properties of the nucleon

- Connected to charge, magnetization distribution
- Crucial testing ground for models of the nucleon internal structure



The nucleon **electromagnetic vertex** Γ_μ describing the hadron current:

$$\Gamma_\mu(p', p) = \gamma_\mu F_1(q^2) + \frac{i\sigma_{\mu\nu} q^\nu}{2m_p} F_2(q^2)$$

Sachs FFs: $G_E(q^2) = F_1(q^2) + \tau \kappa_p F_2(q^2)$, $G_M(q^2) = F_1(q^2) + \kappa_p F_2(q^2)$

Normalization of FF: $q^2 = 0: G_E = F_1(0), G_M = \mu_N$ $q^2 = 4m_N^2: G_E = G_M$

Pair production of baryon

EMFFs parameterize the pair production cross section in e^+e^-

$$\frac{d\sigma_{B\bar{B}}(s)}{d\Omega} = \frac{\alpha^2\beta C}{4s} \left[|G_M(s)|^2(1 + \cos^2\theta) + \frac{4m_B^2}{s} |G_E(s)|^2 \sin^2\theta \right] \equiv N_0(1 + \alpha_B \sin^2\theta)$$

Ratio $R_{em} = |G_E/G_M|$ reflects polar angle distribution of produced baryon!

$|G_E|$ and $|G_M|$ can be separately evaluated after determining N_0 and α_B .

After the integration over the polar angle θ

$$\sigma_{B\bar{B}}(s) = \frac{4\pi\alpha^2\beta C}{3s} \left[|G_M(s)|^2 + \frac{2m_B^2}{s} |G_E(s)|^2 \right]$$

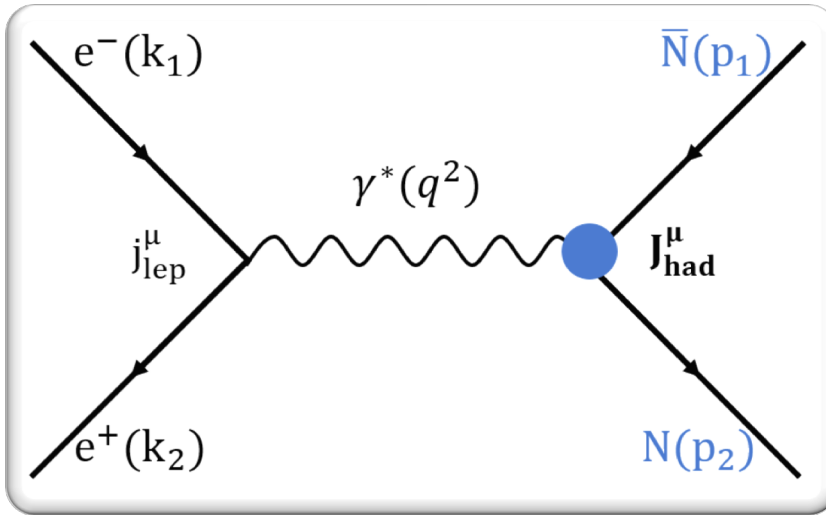
The so-called effective form factor could be defined in terms of EMFFs:

$$|G_{\text{eff}}(s)| = \sqrt{\frac{\sigma_{B\bar{B}}(s)}{\frac{4\pi\alpha^2\beta C}{3s} \left(1 + \frac{2m_B^2}{s}\right)}} = \sqrt{\frac{|G_M(s)|^2 + \frac{2m_B^2}{s} |G_E(s)|^2}{1 + \frac{2m_B^2}{s}}}$$

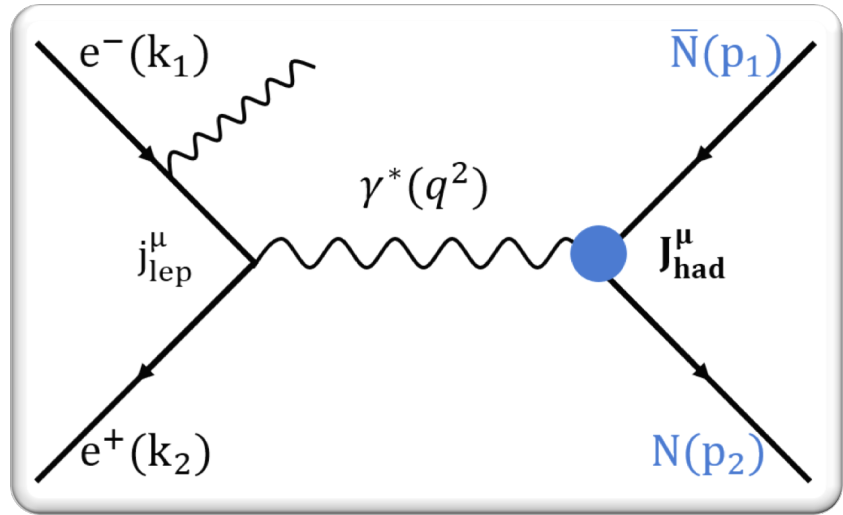
Effective FF reflects the magnitude of production cross section of baryon!

Experimental access of Time-like form factors

Energy scan

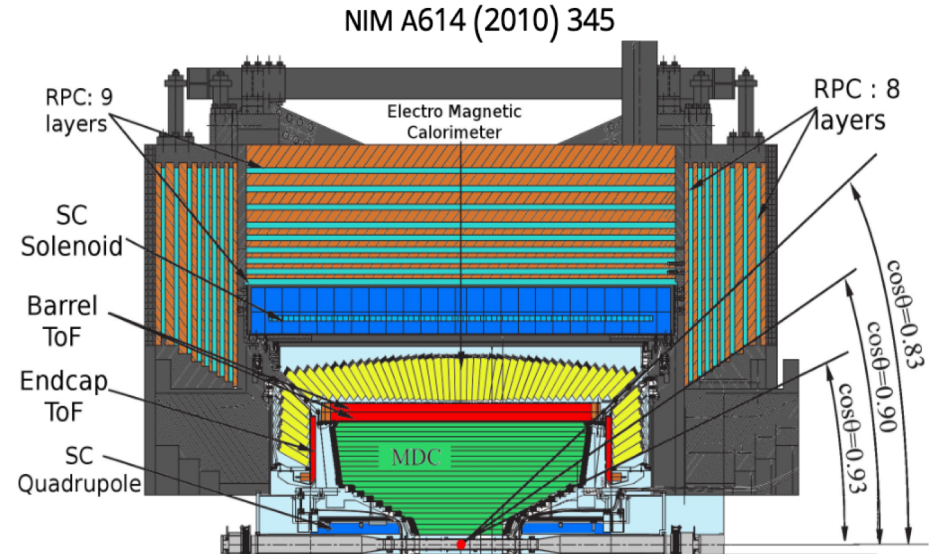


Initial-state-radiation



	Energy Scan	Initial State Radiation
E_{beam}	discrete	fixed
\mathcal{L}	low at each beam energy	high at one beam energy
σ	$\frac{d\sigma_{p\bar{p}}}{d(\cos\theta)} = \frac{\alpha^2\beta C}{4q^2} [G_M ^2(1 + \cos^2\theta) + \frac{4m_p^2}{q^2} G_E ^2 \sin^2\theta]$	$\frac{d^2\sigma_{p\bar{p}\gamma}}{dx d\theta_\gamma} = W(s, x, \theta_\gamma) \sigma_{p\bar{p}}(q^2)$ $W(s, x, \theta_\gamma) = \frac{\alpha}{\pi x} \left(\frac{2-2x+x^2}{\sin^2\theta_\gamma} - \frac{x^2}{2} \right)$
q^2	single at each beam energy	from threshold to s

BEPCII and BESIII



- Located at the BEPCII collider (Beijing/China)
- Symmetric beams (2-5 GeV C.M. Energy)
- Maximum Luminosity: $1 \text{ nb}^{-1}/\text{s}$
- 93% coverage of the solid angle

Superconducting Solenoid:

- 1T magnetic field

Time-of-Flight System:

- 90 – 110 ps resolution

Drift Chamber:

- 0.5% momentum resolution
- 6% dE/dx resolution

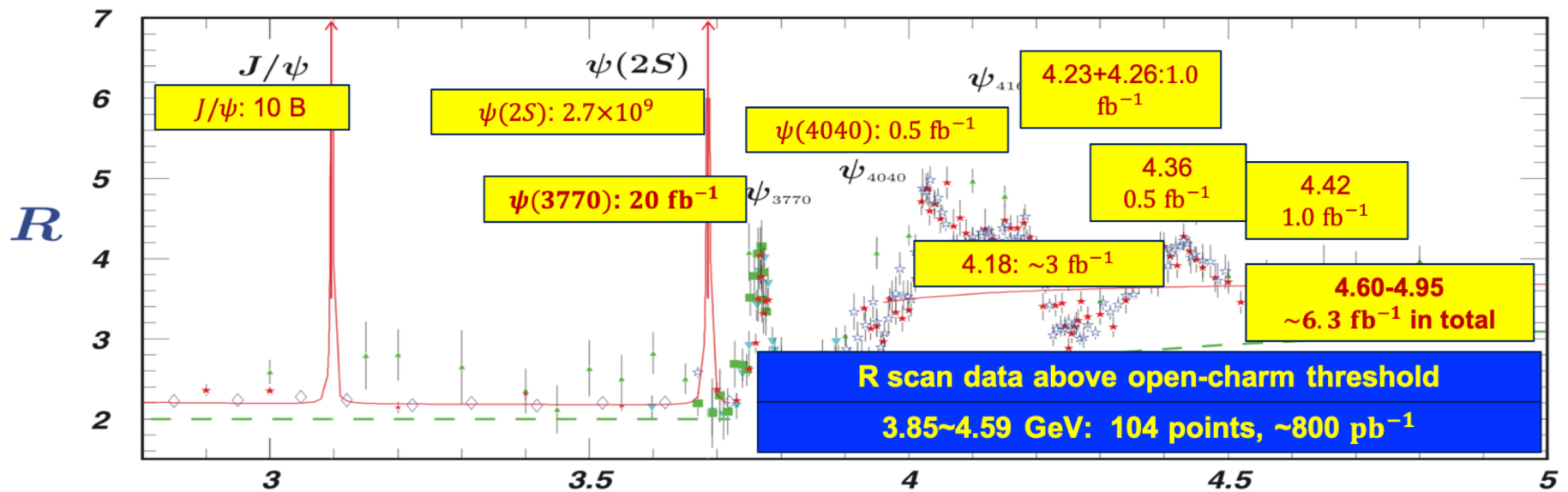
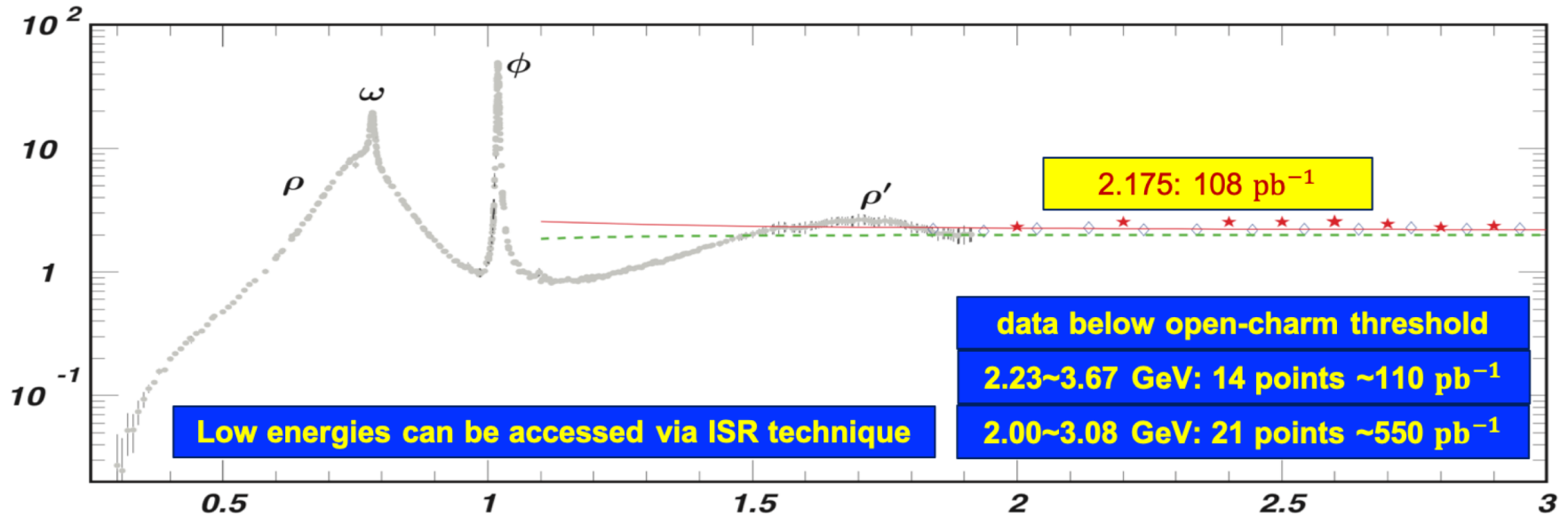
Muon Chambers:

- 8-9 layers of RPCs
- 1.4-1.7 cm resolution
- $P > 400 \text{ MeV}$

Electromagnetic Calorimeter:

- 6240 CsI(Tl) crystals
- 2.5% energy resolution
- 0.5 – 0.7 cm spatial resolution

Data collected at BESIII

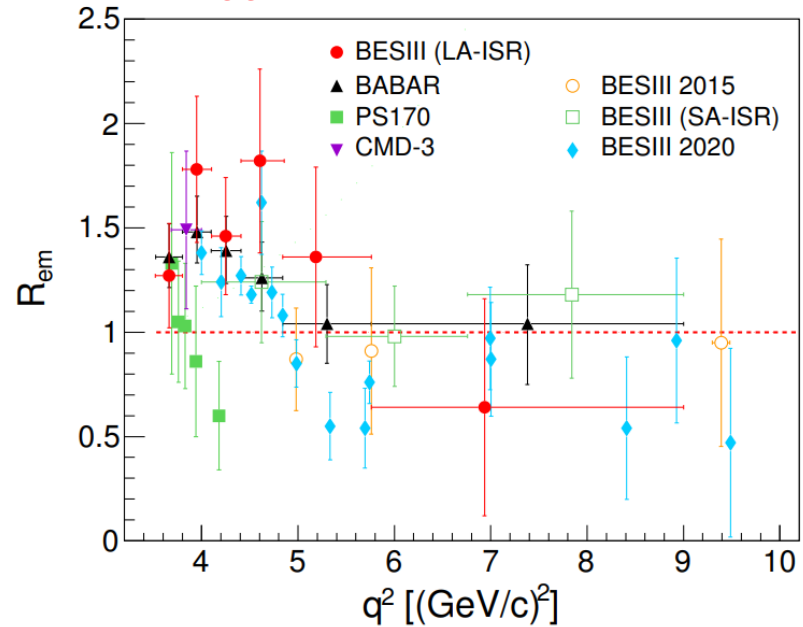
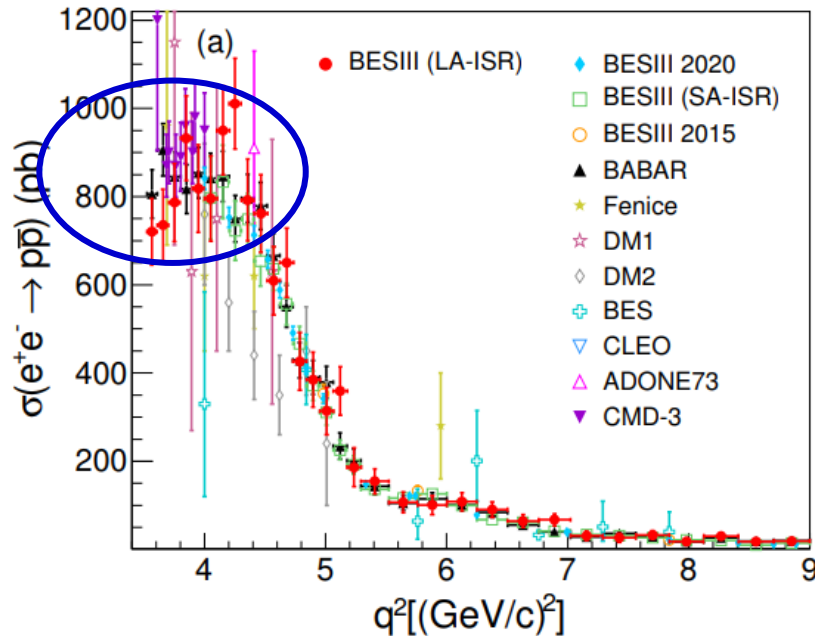


Proton form factors

ISR approach with detected and undetected ISR photon using BESIII data corresponds to 7.5 fb^{-1} integrated luminosity.

SA-ISR(un-tagged): PRD 99, 092002 (2019)

LA-ISR(tagged): PLB 817, 136328 (2019)



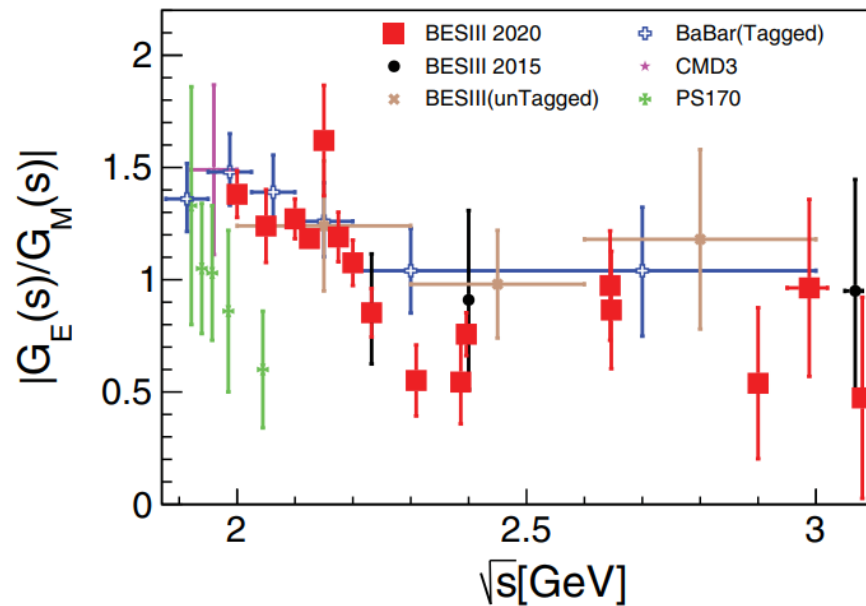
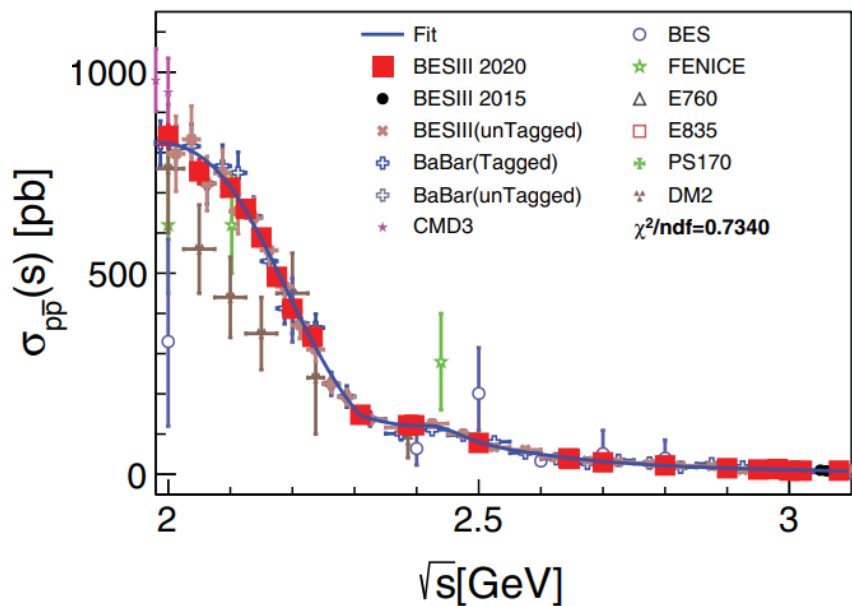
➤ From threshold to $q^2 = 4.0 \text{ GeV}^2$, average cross section 840 pb

➤ **Point-like** cross section at threshold, $\sigma_{\text{point}} = \frac{\pi\alpha^2}{3m_B^2\tau} \left[1 + \frac{1}{2\tau} \right] = 845 \text{ pb}$

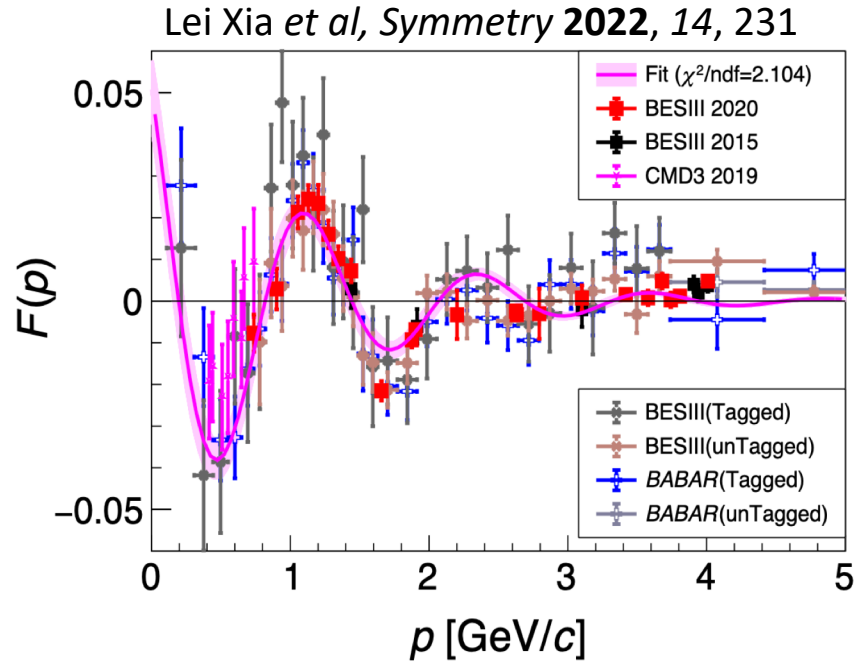
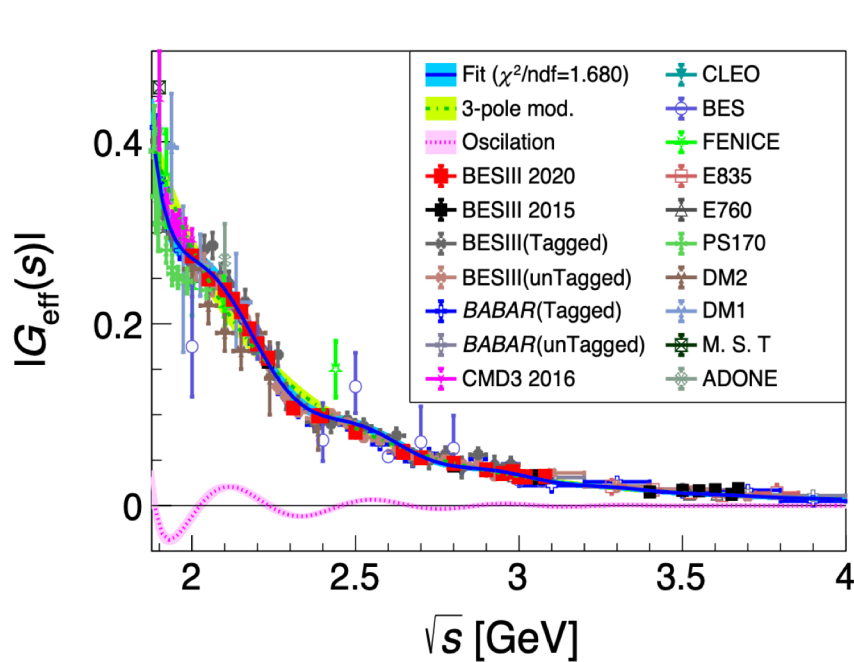
Proton form factors

- Scan technique from 2.00 to 3.08 GeV at BESIII, using data of 688.5 pb^{-1}
- $|G_E/G_M|$ is determined with **high accuracy**, comparable with space-like region.
- $|G_E|$ and $|G_M|$ are separated by analyzing the polar angle distribution.

PRL 124, 042001 (2020)
PRD 91, 112004 (2015)



Oscillation feature confirmed in $|G_{\text{eff}}|$

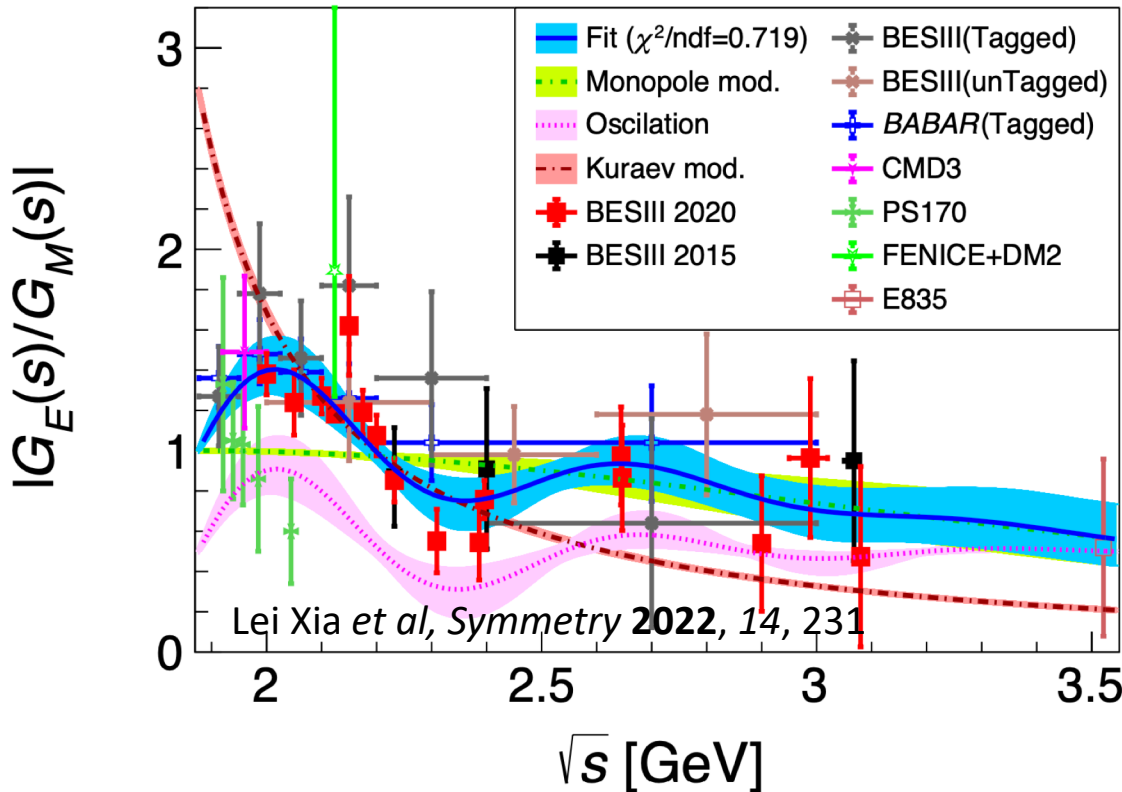


$|G_{\text{eff}}|$ data are fitted with the model: the **monopole decrease** with a **damped oscillation** : *E. Tomasi-Gustafsson et al., PRL. 114, 232301 (2015), PRC 103, 035203 (2021)*

$$|G_{\text{eff}}|(s) = \frac{\mathcal{A}}{\left(1 + \frac{s}{a_0}\right) \left(1 - \frac{s}{0.71 \text{ GeV}^2}\right)^2} + b_0 e^{-b_1 p(s)} \cos[b_2 p(s) + b_3]$$

Oscillation feature in the cross section line-shape!

Oscillation feature in $|G_E/G_M|$



$|G_E/G_M|$ data can be well described by a function combining the **monopole decrease** with a **damped oscillation**

oscillation feature in the polar angle distribution of the outgoing proton!

$|G_E/G_M|$ data are fitted with the model:

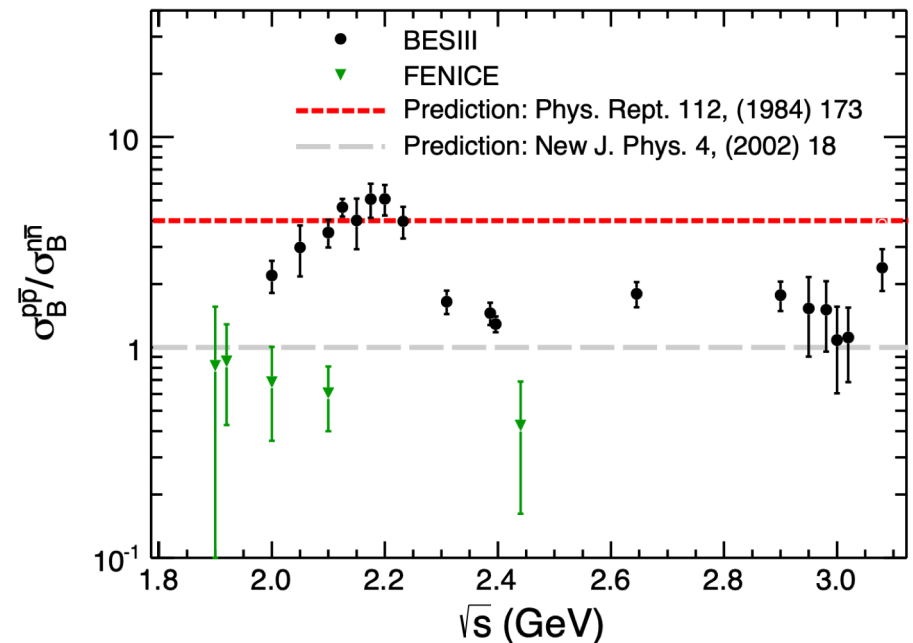
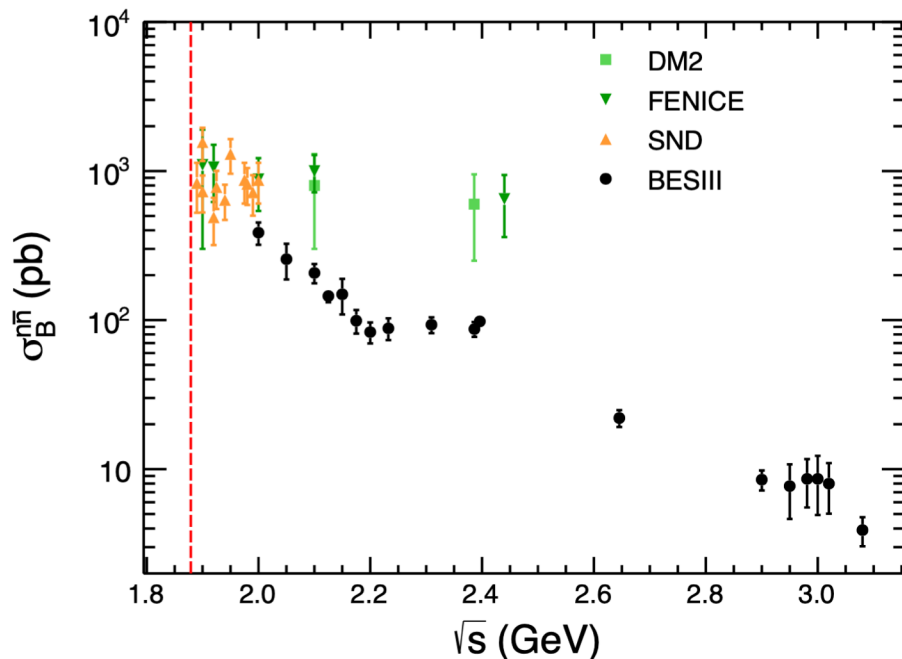
$$|G_E/G_M|(s) = \frac{1}{1 + \omega^2(s)/r_0} \left[1 + r_1 e^{-r_2 \omega(s)} \sin(r_3 \omega(s)) \right]$$

E. Tomasi-Gustafsson et al., *PRL*. 114, 232301 (2015), *PRC* 103, 035203 (2021)

Neutron form factors

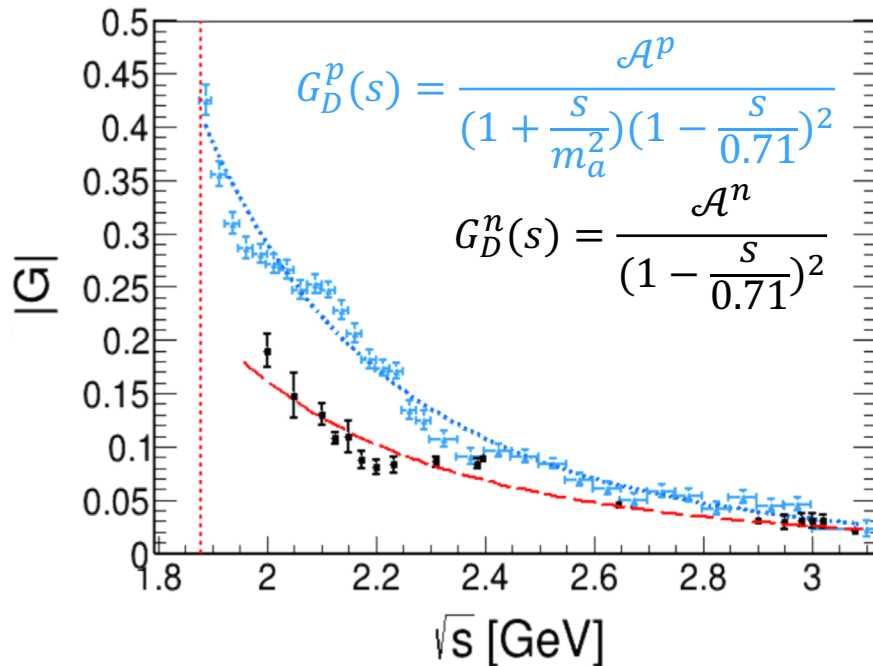
- Scan technique from 2.00 to 3.08 GeV at BESIII, using data of 647.9 pb^{-1}
- Unprecedented precision achieved, smaller than 8% at 2.396 GeV
- Clearly clarify the “puzzle” that photon-neutron coupling larger than photon-proton coupling which exists over 20 years.

Nature Phys. 17 (2021) 11, 1200-1204

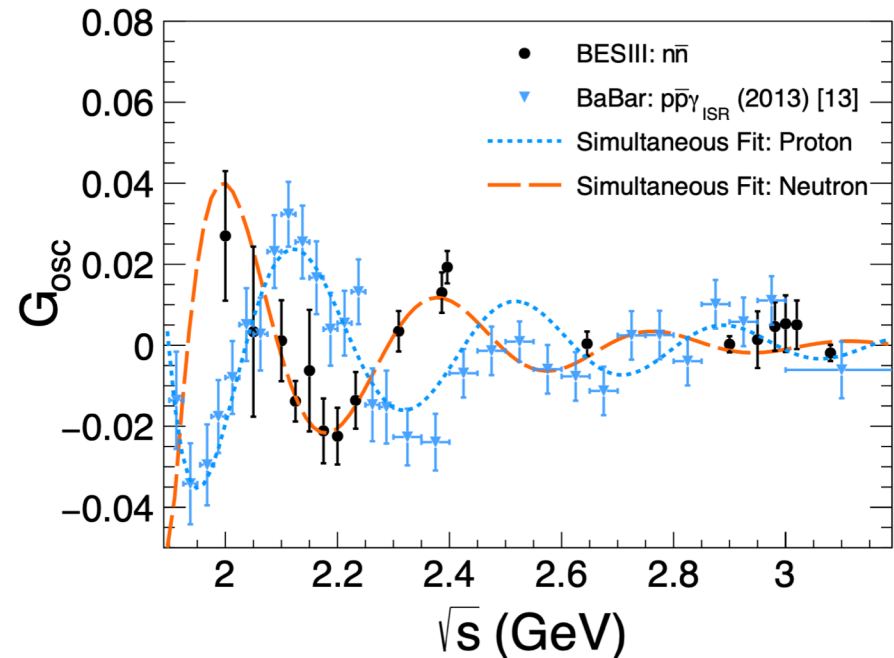


Oscillation feature in $|G_{\text{eff}}|$

- Oscillation in addition to the dipole law: $|G_{\text{eff}}^{p,n}(s)| = G_D^{p,n}(s) + G_{\text{osc}}^{p,n}(s)$
- Simultaneous fit on proton and neutron data with the same frequency but different phase: $G_{\text{osc}}^{p,n}(s) = b_0^{p,n} e^{-b_1^{p,n} p(s)} \cos[b_2 p(s) + b_3^{p,n}]$
- Fitted well but a phase shift around $(125 \pm 12)^\circ$ is observed

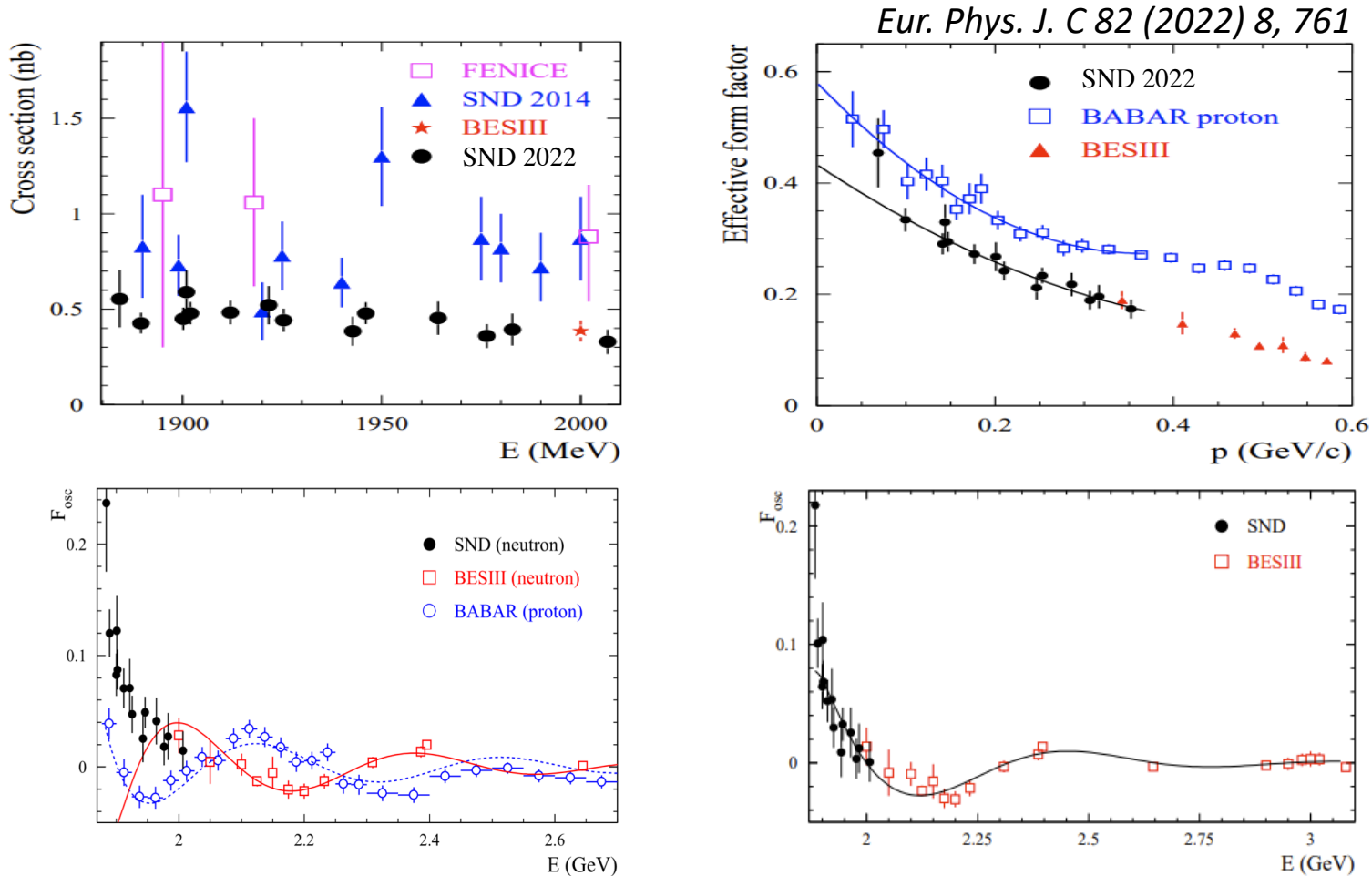


Nature Phys. 17 (2021) 11, 1200-1204



Oscillation feature in $|G_{\text{eff}}|$

Recent SND measurement suggests a different frequency:

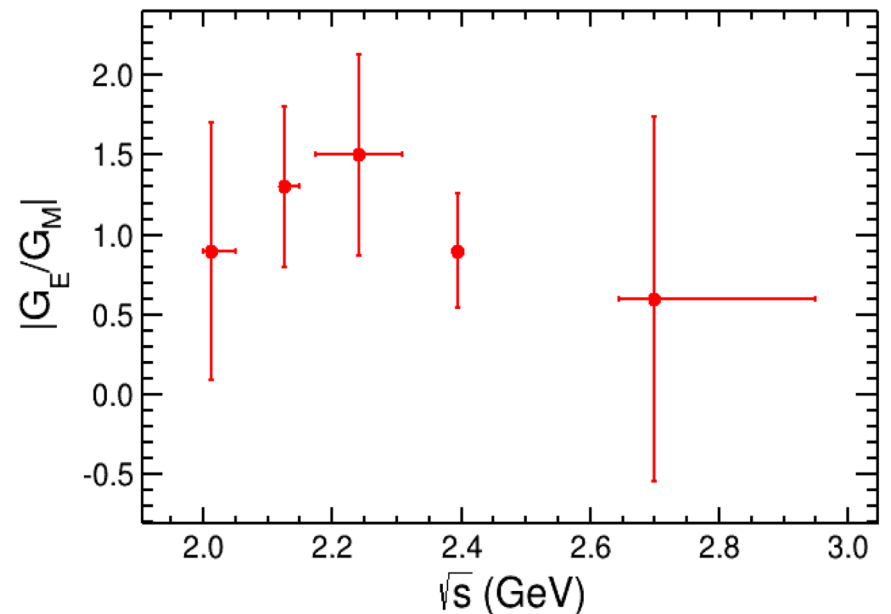
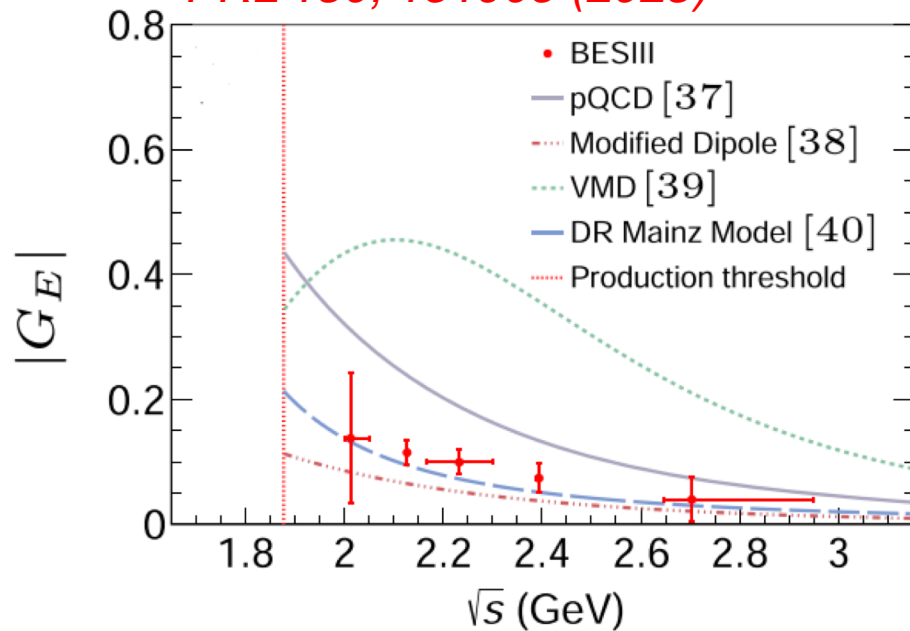


Additional experimental and theoretical inputs are desired!

$|G_E|$ and $|G_M|$ of neutron

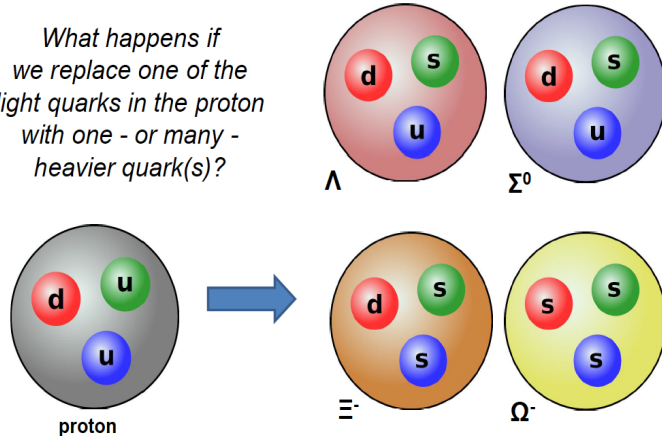
- $|G_E|$ and $|G_M|$ are obtained in **5 energy intervals** due to the limited statistics, $|G_E/G_M|$ distribution is not shown in the paper
- BESIII $|G_M|$ values are smaller than that of FENICE by a factor of 2-3
- Data is compared with various models: pQCD, modified dipole, VMD and dispersion relations (DR), where the DR model gives good consistency

PRL 130, 151905 (2023)

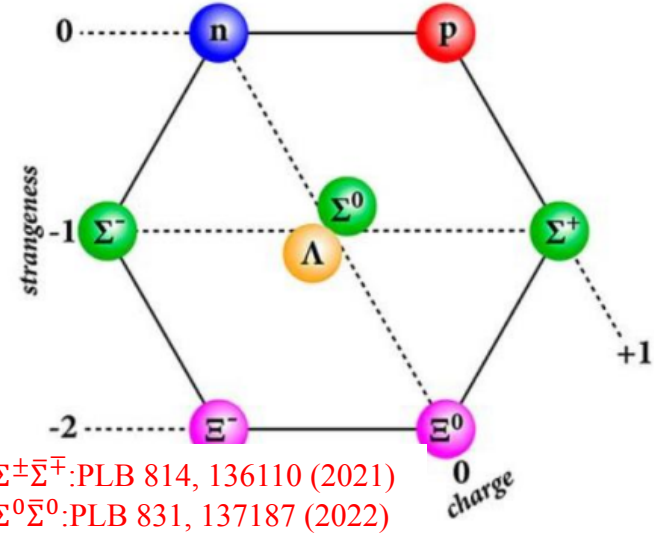
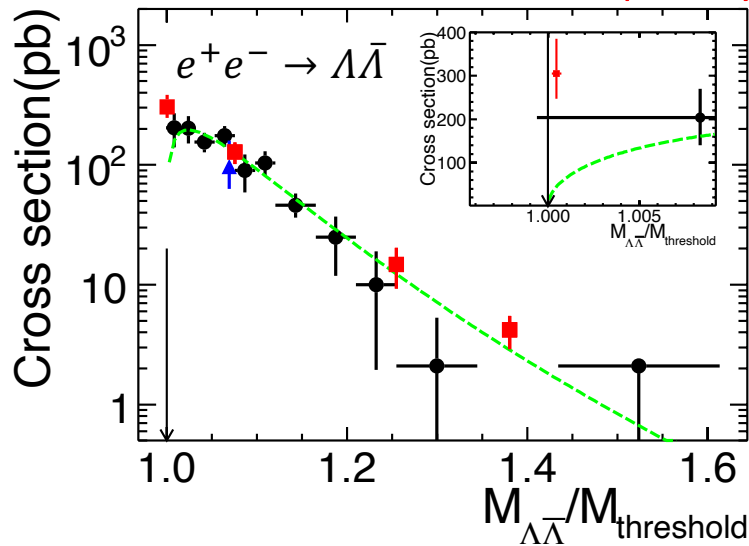


Production cross section of hyperons

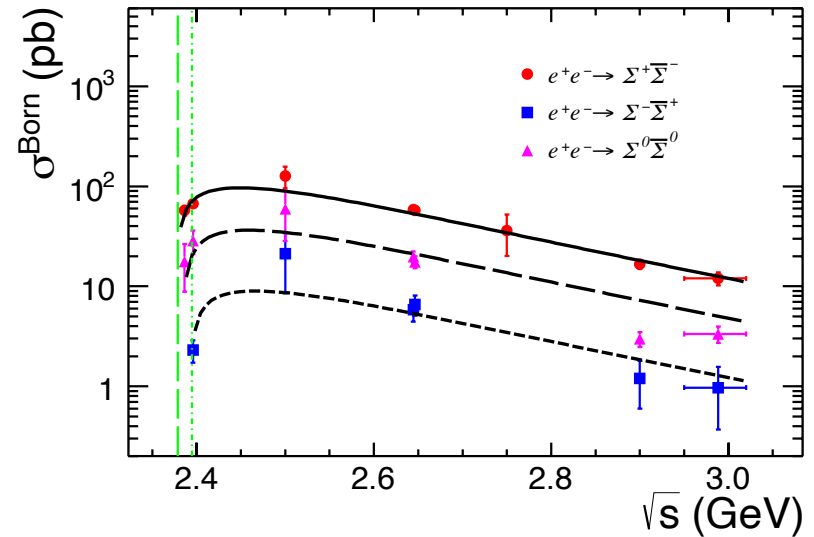
What happens if we replace one of the light quarks in the proton with one - or many - heavier quark(s)?



PRD 97, 032013 (2018)



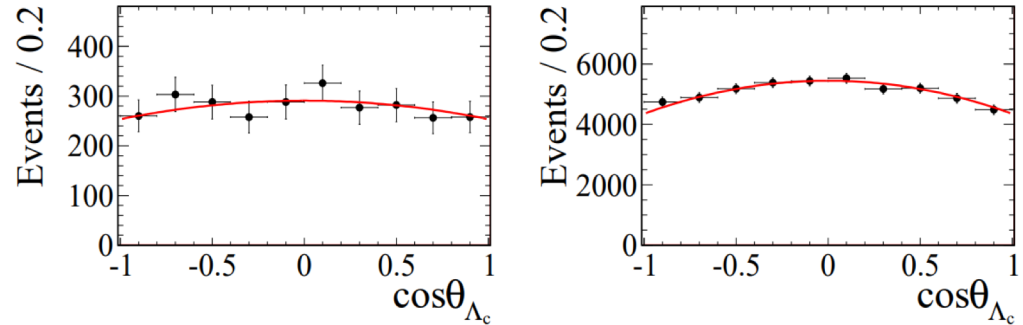
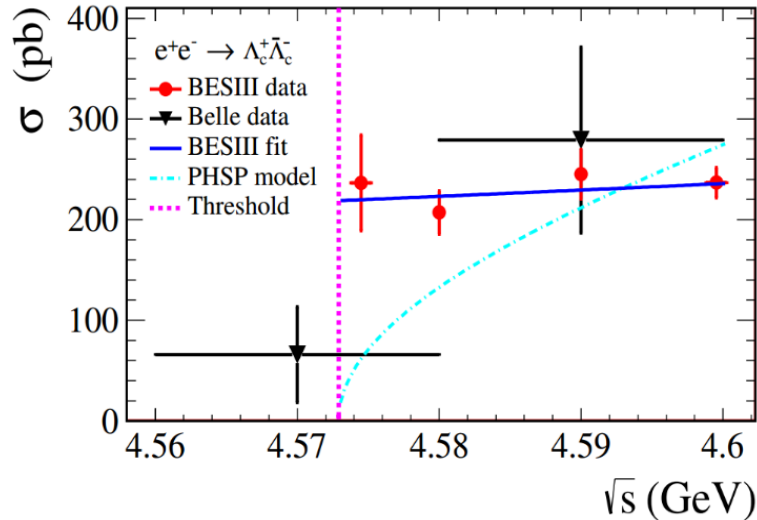
$\Sigma^\pm\bar{\Sigma}^\mp$: PLB 814, 136110 (2021)
 $\Sigma^0\bar{\Sigma}^0$: PLB 831, 137187 (2022)



EMFF data of hyperon is limited due to the small statistics

Production of charmed hyperon

BESIII measured the production of Λ_c near-threshold:



\sqrt{s} (MeV)	α_{Λ_c}	$ G_E/G_M $
4574.5	$-0.13 \pm 0.12 \pm 0.08$	$1.14 \pm 0.14 \pm 0.07$
4599.5	$-0.20 \pm 0.04 \pm 0.02$	$1.23 \pm 0.05 \pm 0.03$

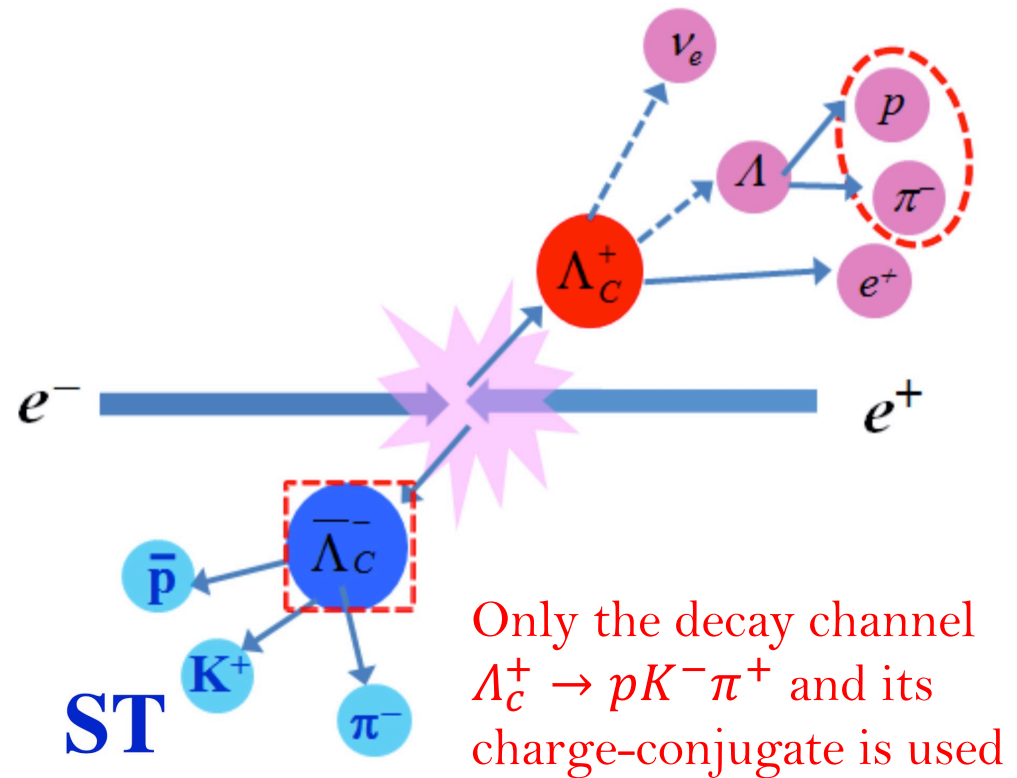
- Precise **non-zero cross section** near the kinematic threshold, a significantly different energy-dependent trend from Belle's measurement
- $|G_E/G_M|$ is **consistent with 1** near the kinematic threshold
- Results are limited in a narrow c.m. energy region near threshold

A thorough study of the cross section and EMFFs is needed!

Cross section and EMFF measurements of Λ_c^+

A combined approach of the single tag (ST) and double tag (DT):

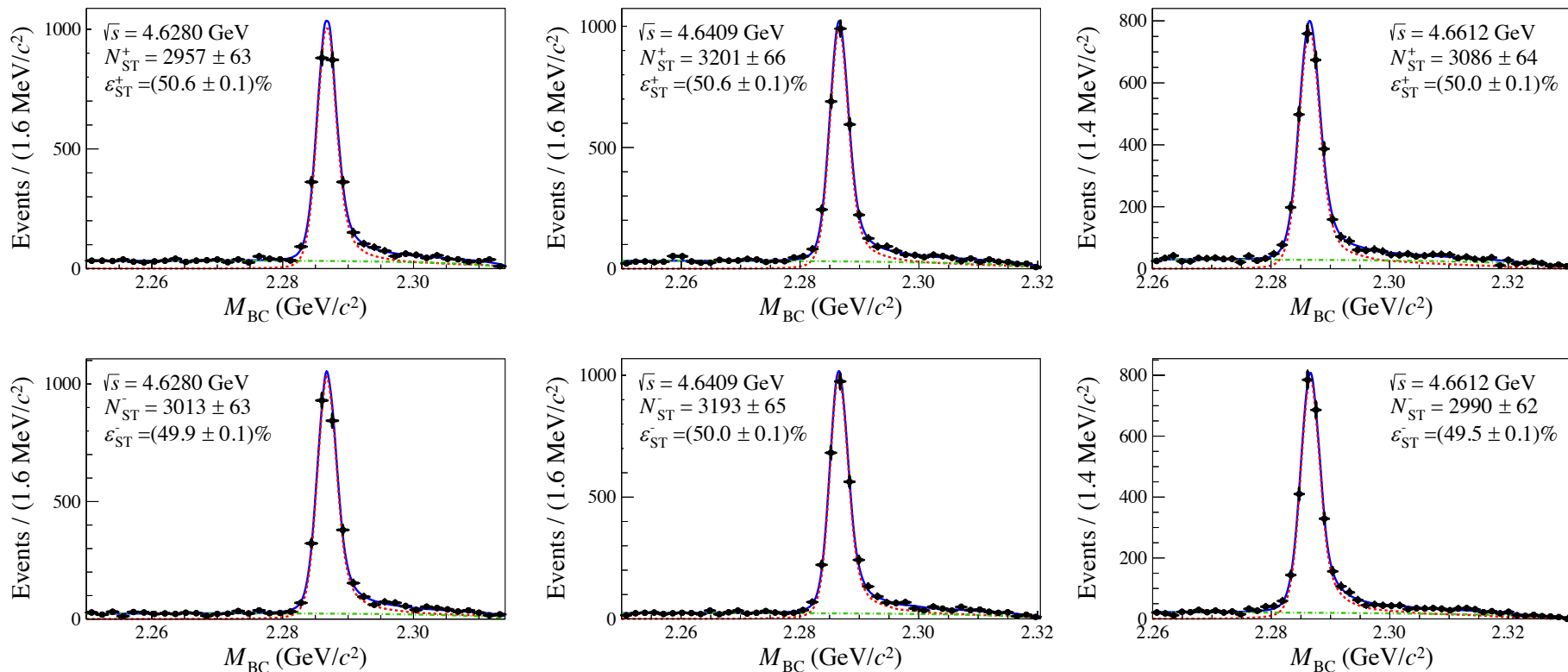
\sqrt{s} (GeV)	\mathcal{L}_{int} (pb^{-1})
4.6119	103.83
4.6280	521.52
4.6409	552.41
4.6612	529.63
4.6819	1669.31
4.6988	536.45
4.7397	164.27
4.7500	367.21
4.7805	512.78
4.8431	527.29
4.9180	208.11
4.9509	160.37



Sufficient statistics enable a DT analysis to reduce uncertainty!

Production cross section of Λ_c^+

Significant positive and negative ST yields in the Y(4630) region:



Flat energy-dependent L_{int} , ST yields, and efficiency results in flat cross section

Production cross section of Λ_c^+

The Born cross section of channel $\Lambda_c^+ \rightarrow pK^-\pi^+$ and $\bar{\Lambda}_c^- \rightarrow \bar{p}K^+\pi^-$:

$$\sigma_{\pm} = \frac{N_{ST}^{\pm}}{\varepsilon_{ST}^{\pm} \mathcal{L}_{\text{int}} f_{VP} f_{ISR} \mathcal{B}_{\pm}}$$

$$N_{ST}^{\pm, n} = N_{\Lambda_c^+ \bar{\Lambda}_c^-}^n \varepsilon_{ST}^{\pm, n} \mathcal{B}_{\pm}, \quad N_{DT}^n = N_{\Lambda_c^+ \bar{\Lambda}_c^-}^n \mathcal{B}_+ \mathcal{B}_- \varepsilon_{DT}^n$$

Thus,

$$N_{DT}^n = \mathcal{B}_{\pm} \frac{N_{ST}^{\mp, n} \varepsilon_{DT}^n}{\varepsilon_{ST}^{\mp, n}}, \quad N_{DT} = \sum_{n=1}^9 N_{DT}^n = \mathcal{B}_{\pm} \sum_{n=1}^9 \left(\frac{N_{ST}^{\mp, n} \varepsilon_{DT}^n}{\varepsilon_{ST}^{\mp, n}} \right)$$

As a result

$$\mathcal{B}_{\pm} = N_{DT} / \sum_{n=1}^9 \left(\frac{N_{ST}^{\mp, n} \varepsilon_{DT}^n}{\varepsilon_{ST}^{\mp, n}} \right)$$

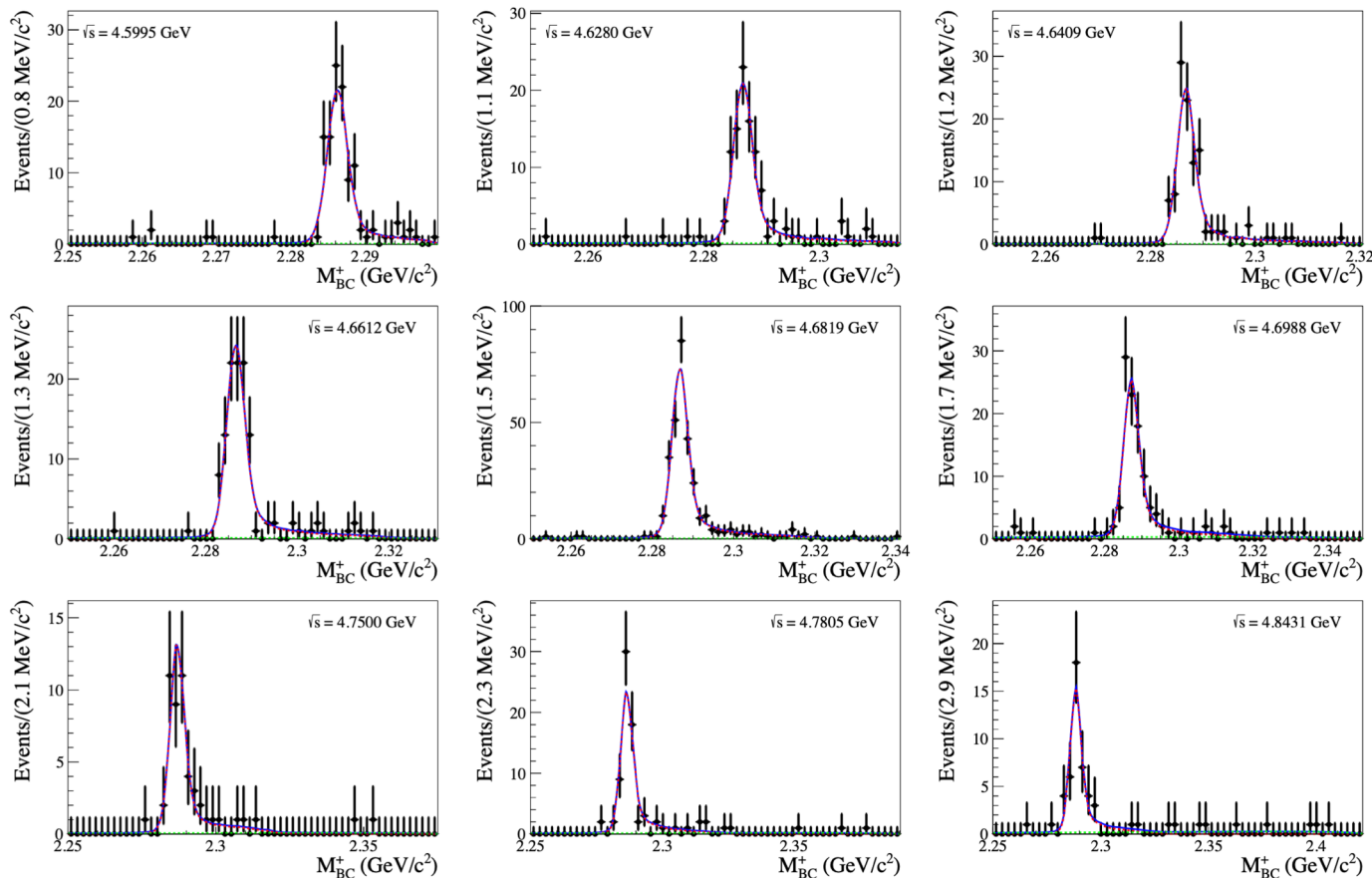
Thus,

$$\sigma_{\pm} = \frac{N_{ST}^{\pm}}{\varepsilon_{ST}^{\pm} \mathcal{L}_{\text{int}} f_{VP} f_{ISR} N_{DT}} \sum_{n=1}^9 \left(\frac{N_{ST}^{\mp, n} \varepsilon_{DT}^n}{\varepsilon_{ST}^{\mp, n}} \right)$$

- Most of the uncertainties in ε_{ST}^{\pm} (due to tracking and PID) are **reduced**.
- The double counting between the uncertainties of ε_{ST}^{\pm} and \mathcal{B}_{\pm} is **avoided**.
- Data samples with $\mathcal{L}_{\text{int}} > 350 \text{ pb}^{-1}$ is used in the double tag analysis.

Production cross section of Λ_c^+

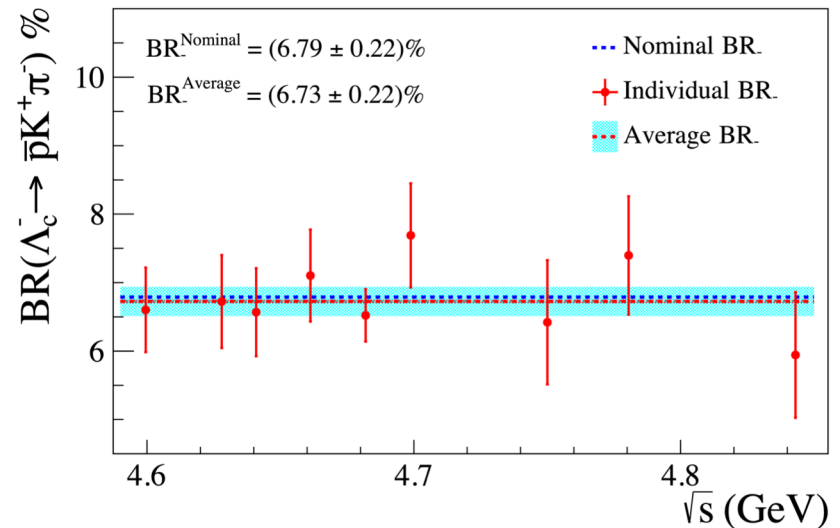
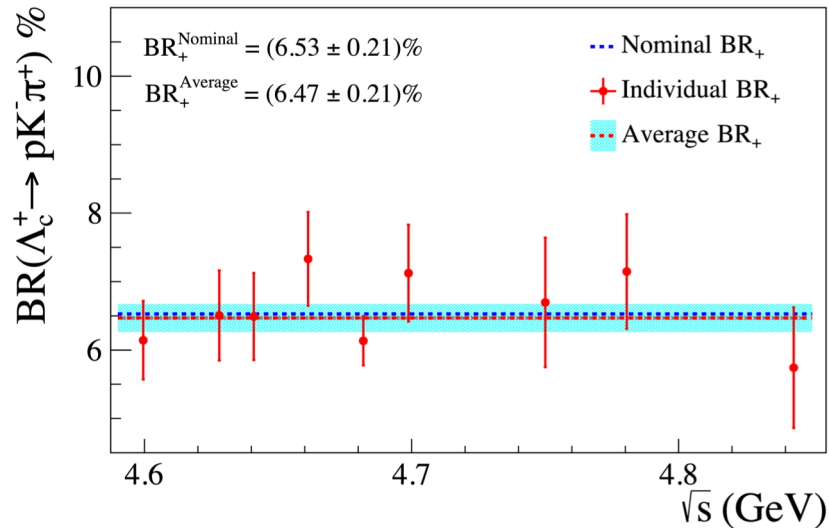
Branching fraction and DT yield is determined by a simultaneous fit:



- A total of **9** data sets are used, small fraction of background events
- \mathcal{B}_{\pm} is the shared parameter in the fit, and \mathcal{B}_+ and \mathcal{B}_- are determined separately

Production cross section of Λ_c^+

To verify the obtained \mathcal{B}_\pm , its energy-dependency is checked:



$$\mathcal{B}_+ = (6.53 \pm 0.21)\%$$

$$\mathcal{B}_- = (6.79 \pm 0.22)\%$$

$$\mathcal{B} = (6.66 \pm 0.22)\%$$

$$N_{\text{DT}} = 1007 \pm 32$$

measurements	$\mathcal{B}(\%)$	Ref. and comments
Belle	$6.84 \pm 0.24^{+0.21}_{-0.27}$	[PRL 113 042002 (2014)]
BESIII 2016	$5.84 \pm 0.27 \pm 0.23$	[PRL 116 052001 (2016)]
PDG	6.26 ± 0.29	[PDG 2023]
BESIII 2023	6.66 ± 0.22	statistical error only

- Systematic uncertainty is reduced by a factor of **2**, i.e., from **6.0%** to **3.2%**
- **Our branching fraction result is consistent with that of Belle!**

Production cross section of Λ_c^+

The Born cross section:

$$\sigma_{\pm} = \frac{N_{\text{ST}}^{\pm}}{\varepsilon_{\text{ST}}^{\pm} \mathcal{L}_{\text{int}} f_{\text{VP}} f_{\text{ISR}} N_{\text{DT}}} \sum_{n=1}^9 \left(\frac{N_{\text{ST}}^{\mp, n} \varepsilon_{\text{DT}}^n}{\varepsilon_{\text{ST}}^{\mp, n}} \right)$$

The average Born cross section:

$$\sigma = \sum_{i=\pm} \omega_i \sigma_i, \omega_i = (1/\Delta\sigma_i^2) / \left(\sum_i 1/\Delta\sigma_i^2 \right)$$

and corresponding uncertainty takes the form

$$\Delta\sigma^2 = \sum_{i,j=\pm} \omega_i (\mathbf{M}^{\sigma})_{ij} \omega_j, \mathbf{M}^{\sigma} = \mathbf{M}_{\text{stat}}^{\sigma} + \mathbf{M}_{\text{syst}}^{\sigma}$$

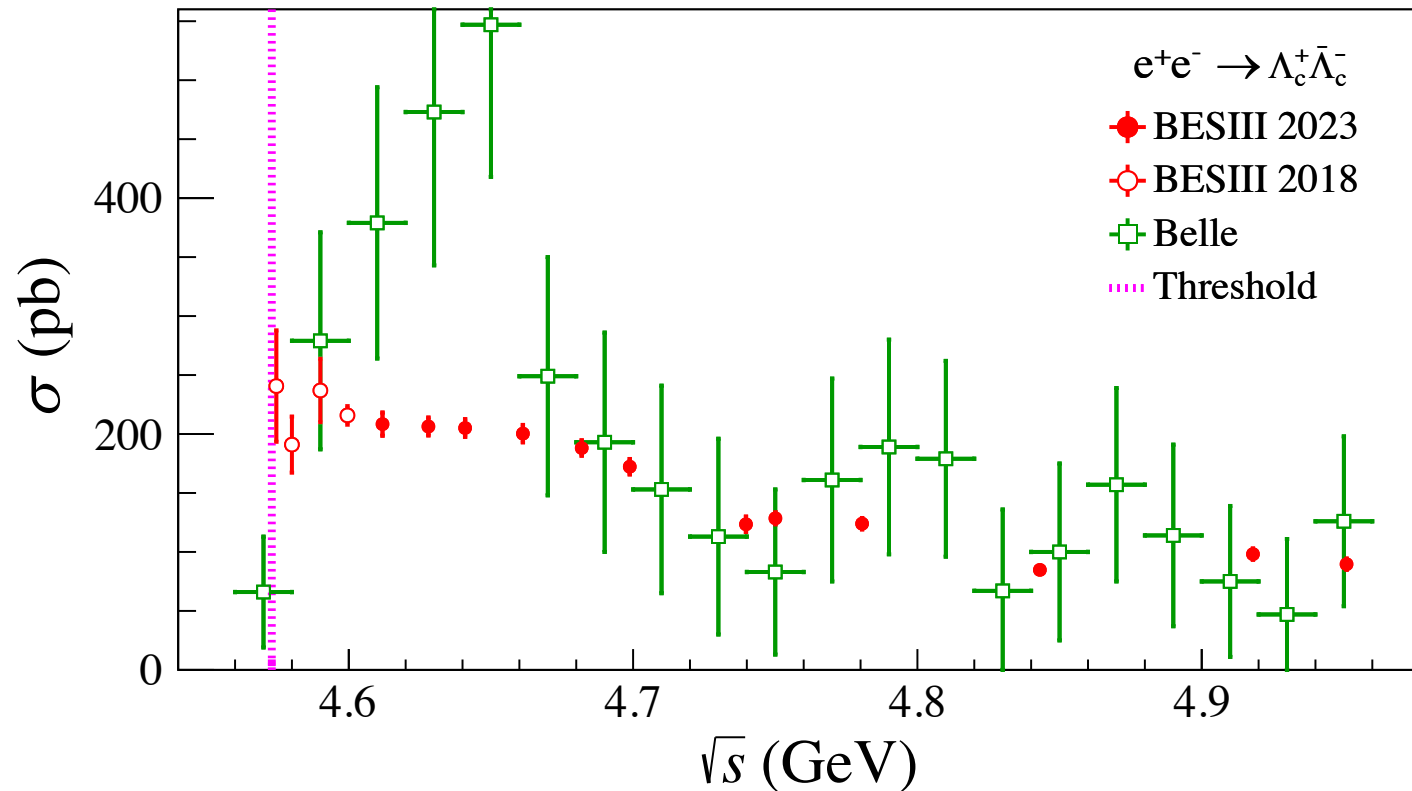
or approximately

$$\Delta\sigma_{\text{stat}}^2 = \sum_{i,j=\pm} \omega_i (\mathbf{M}_{\text{stat}}^{\sigma})_{ij} \omega_j \quad \text{and} \quad \Delta\sigma_{\text{syst}}^2 = \sum_{i,j=\pm} \omega_i (\mathbf{M}_{\text{syst}}^{\sigma})_{ij} \omega_j$$

The covariance matrix \mathbf{M}^{σ} counts for independent and correlated uncertainties.

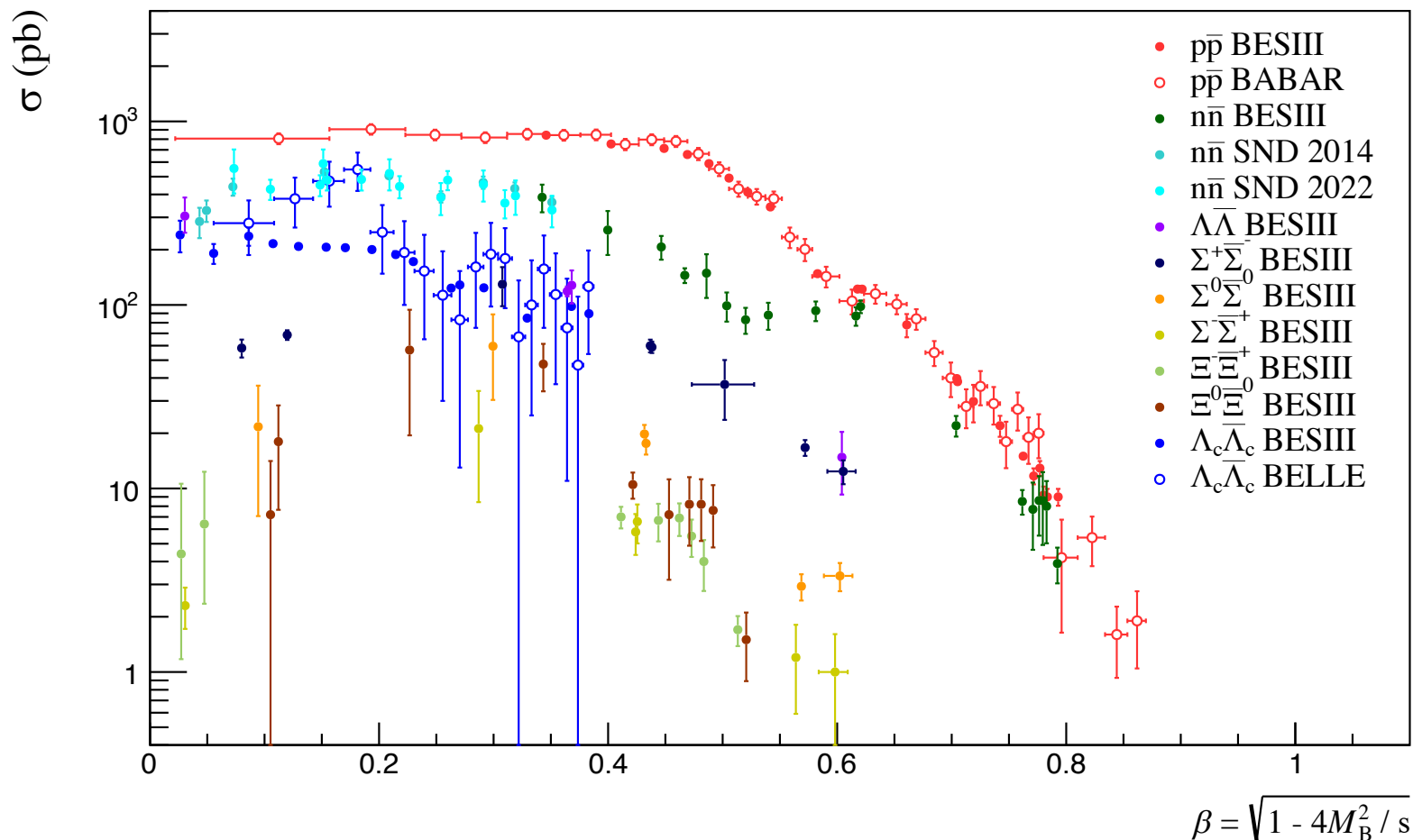
The $i = +, -$ indexed results of tagging $\Lambda_c^+ \rightarrow pK^-\pi^+$ and $\bar{\Lambda}_c^- \rightarrow \bar{p}K^+\pi^-$, respectively.

Production cross section of Λ_c^+



- Typical uncertainty is less than **4.0%**, which is dominated by that of \mathcal{B}_{\pm}
- Cross sections at first four points are re-evaluated using updated \mathcal{L}_{int} and \mathcal{B}_{\pm}
- **Near-threshold cross-section plateau is confirmed up to 4.68 GeV, and no resonance structure is observed around 4.64 GeV -- no charmed baryonium?**

Production cross section of Λ_c^+

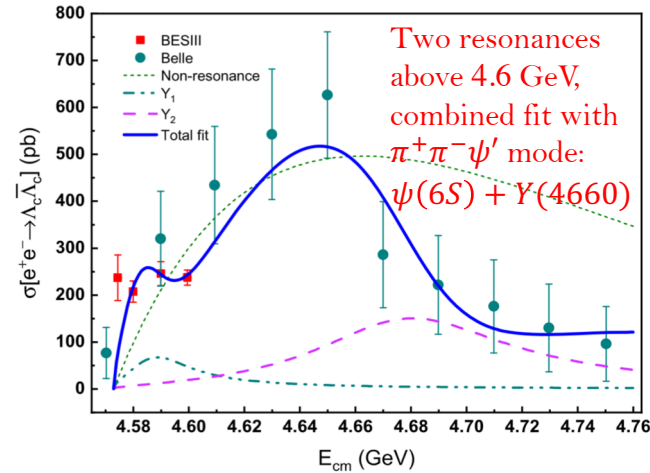
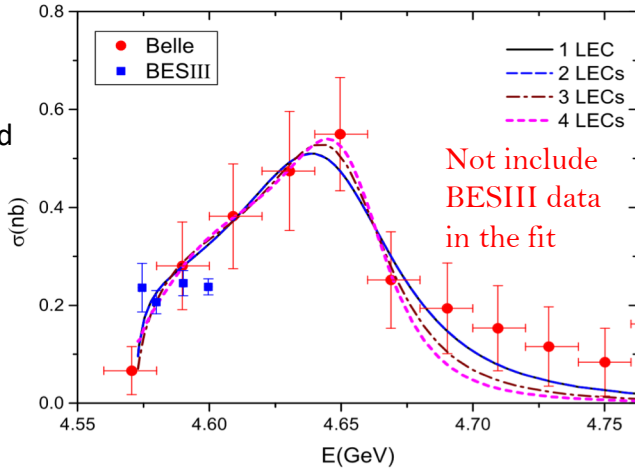


Similar momentum-dependency with the proton and neutron

Discussions in the theoretical point of view

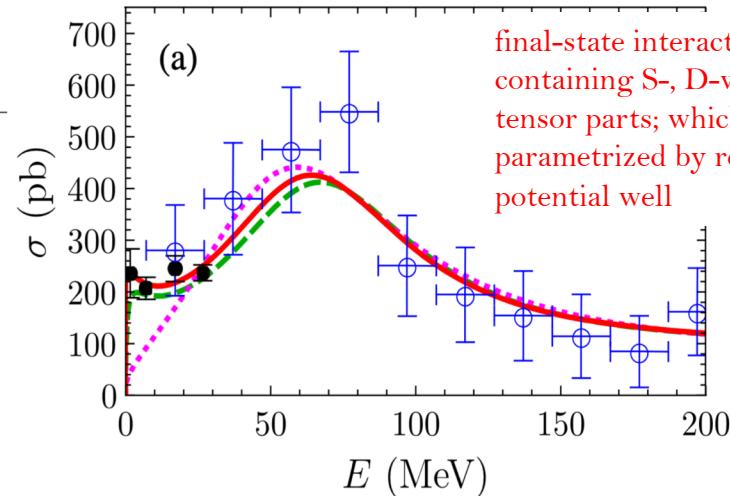
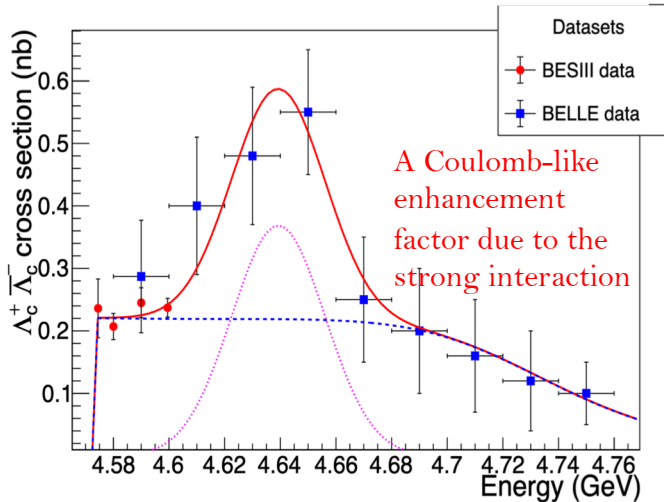
BESIII data affects the parameterization of $Y(4630)$:

Ling-Yun Dai,
Johann
Haidenbauer, and
Ulf-G. Meißner,
PRD **96**, 116001
(2017)



Jun-Zhang Wang,
Ri-Qing Qian,
Xiang Liu, and
Takayuki Matsuki,
PRD **101**, 034001
(2020)

A. Amoroso
et al,
Universe
2021, **7**,
436



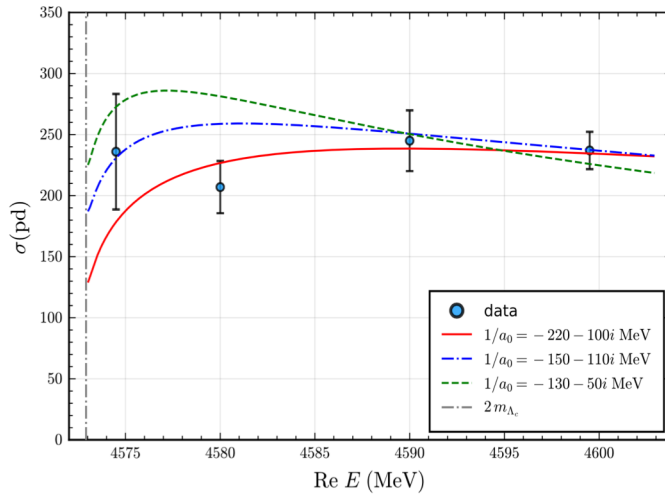
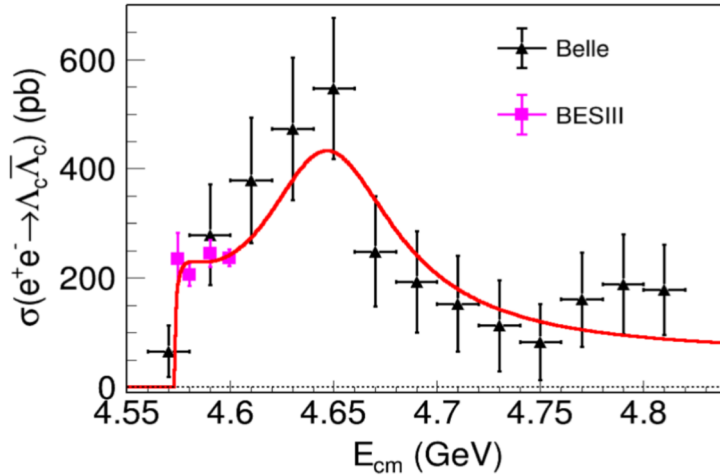
A. I. Milstein and
S. G. Salnikov,
PRD **105**, 074002
(2022)

A plenty of theoretical models are triggered by BESIII data!

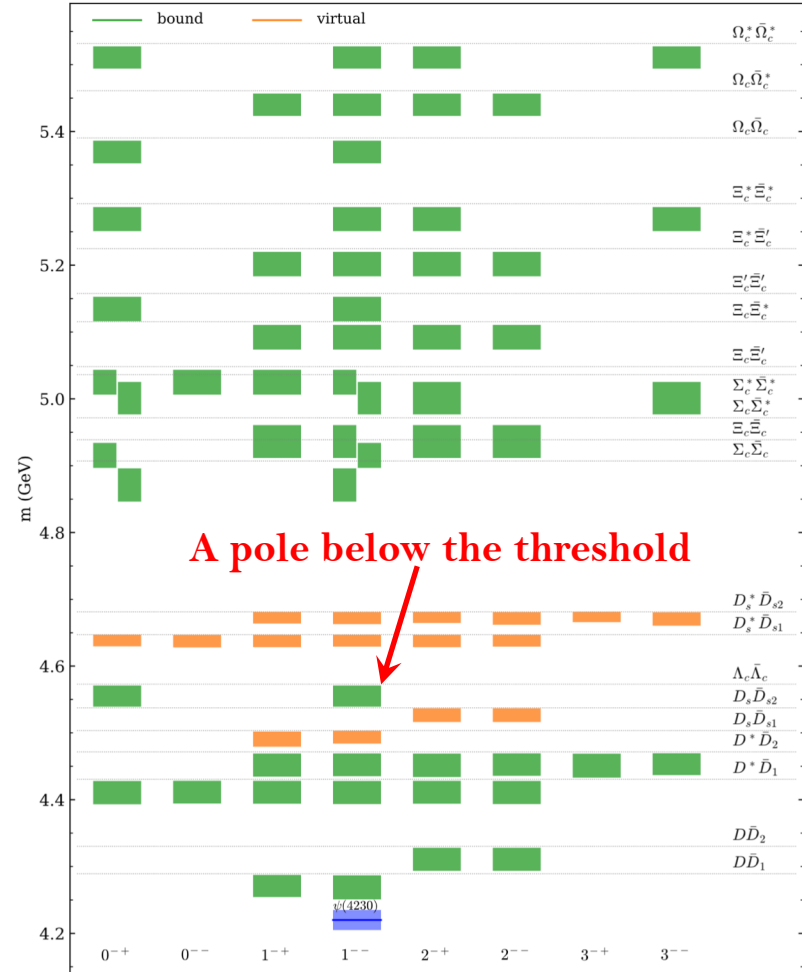
Discussions in the theoretical point of view

BESIII data affects the parameterization of $Y(4630)$:

Qin-Fang Cao, Hong-Rong Qi, Yu-Fei Wang,
and Han-Qing Zheng, PRD **100**, 054040 (2019)



Xiang-Kun Dong, Feng-Kun Guo, and Bing-Song Zou,
Progr. Phys. **41** (2021) 65-93



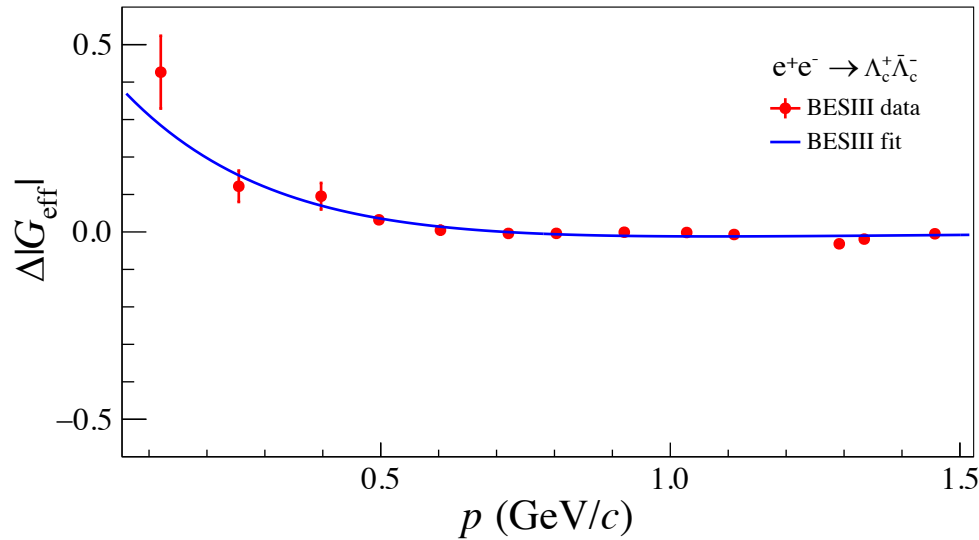
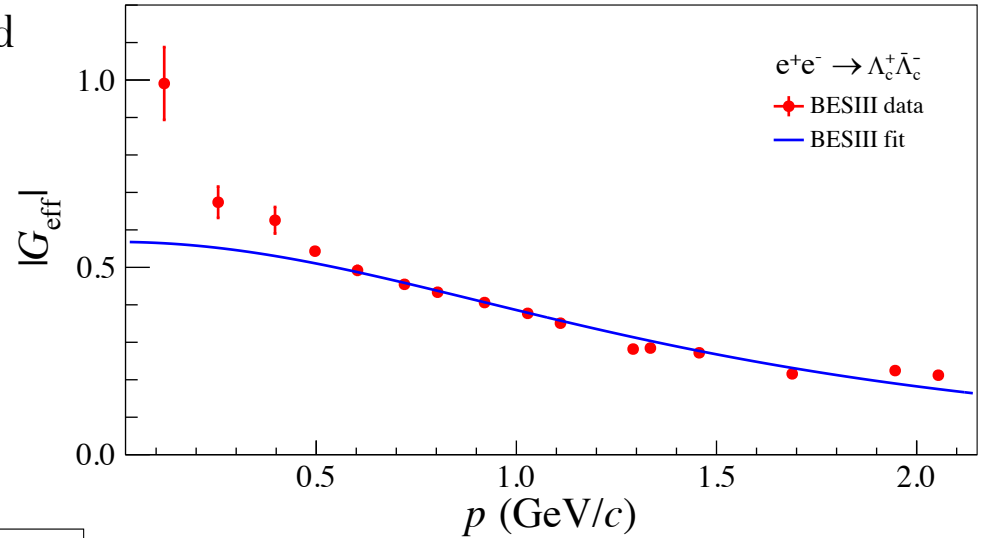
Effective form factor of Λ_c^+

The effective form factors spectrum is fitted with a three-pole model:

$$G_{3p}(s) = \frac{g}{\left(1 + \frac{s}{g_a}\right) \left(1 - \frac{s}{g_b}\right)^2}$$

where

$$p = \sqrt{\left(\frac{s}{2m_{\Lambda_c^+}} - m_{\Lambda_c^+}\right)^2 - m_{\Lambda_c^+}^2}$$



The residual between effective form factors data and the three-pole model is obtained:

$$\Delta|G_{\text{eff}}|(p) = |G_{\text{eff}}|(p) - G_{3p}(p)$$

and fitted to a damped oscillation model:

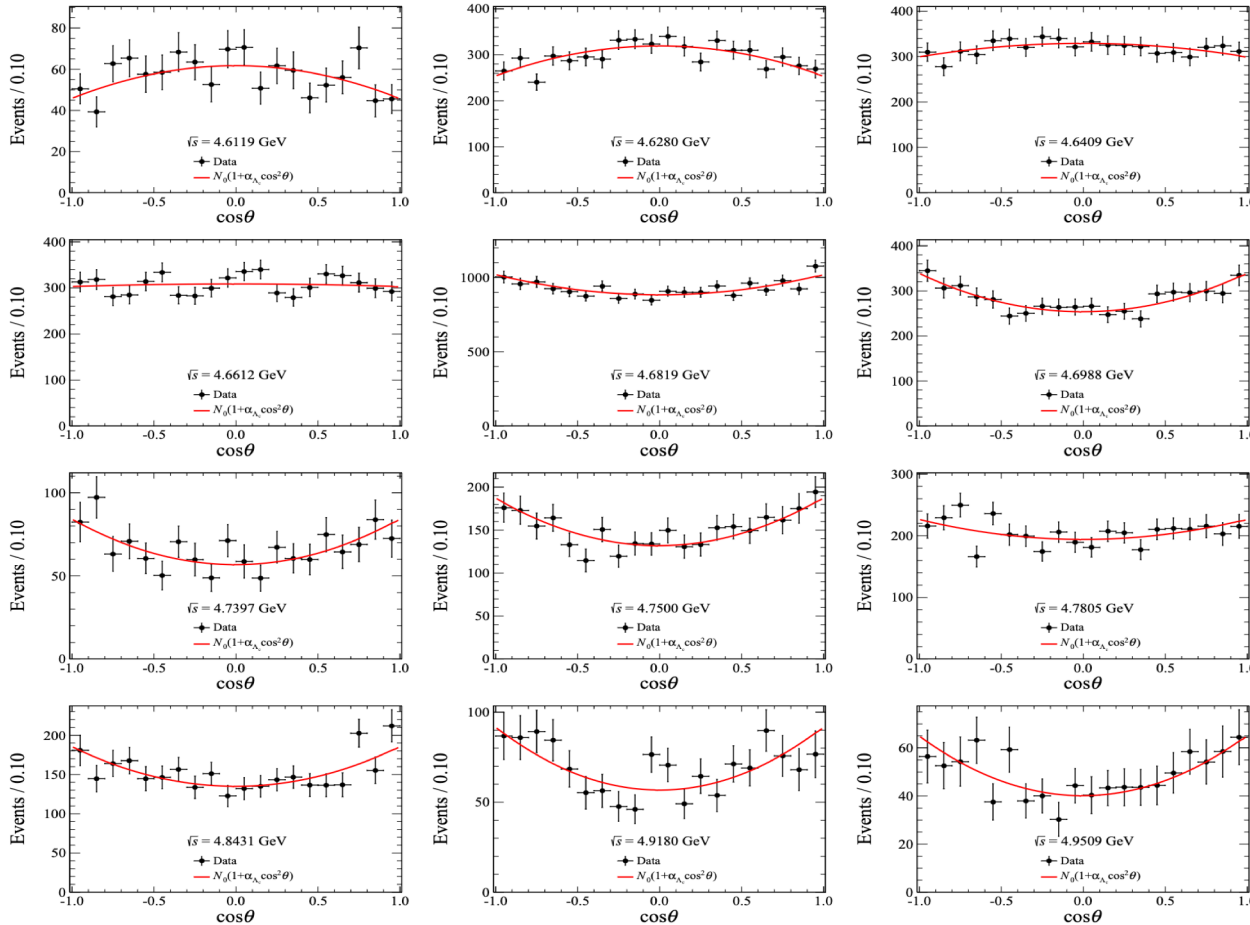
$$|G_{\text{osc}}|(p) = Ae^{-Bp} \cos(Cp + D)$$

$$C = (0.03 \pm 0.14) (\text{GeV}/c)^{-1}$$

No oscillation feature is discerned in the effective form-factor spectrum of Λ_c^+

Electromagnetic form factor of Λ_c^+

The $|G_E/G_M|$ of Λ_c^+ is studied by analyzing the polar angle distribution:



➤ One-photon exchange process is assumed

➤ An ISR correction is considered due to the contribution from ISR returned events

➤ Polar angle spectra is fitted with formula:

$$f(\cos\theta) \propto N_0(1 + \alpha_{\Lambda_c} \cos^2\theta)$$

$$|G_E/G_M|^2 = \frac{s}{4m_{\Lambda_c}^2} \left(\frac{1 - \alpha_{\Lambda_c}}{1 + \alpha_{\Lambda_c}} \right)$$

The reversal of the angular distribution leads to $|G_E/G_M| < 1$

Electromagnetic form factor of Λ_c^+

Additional efforts are made to verify the angular analysis:

- Contribution from **two-photon exchange (TPE)** process is studied via the formula

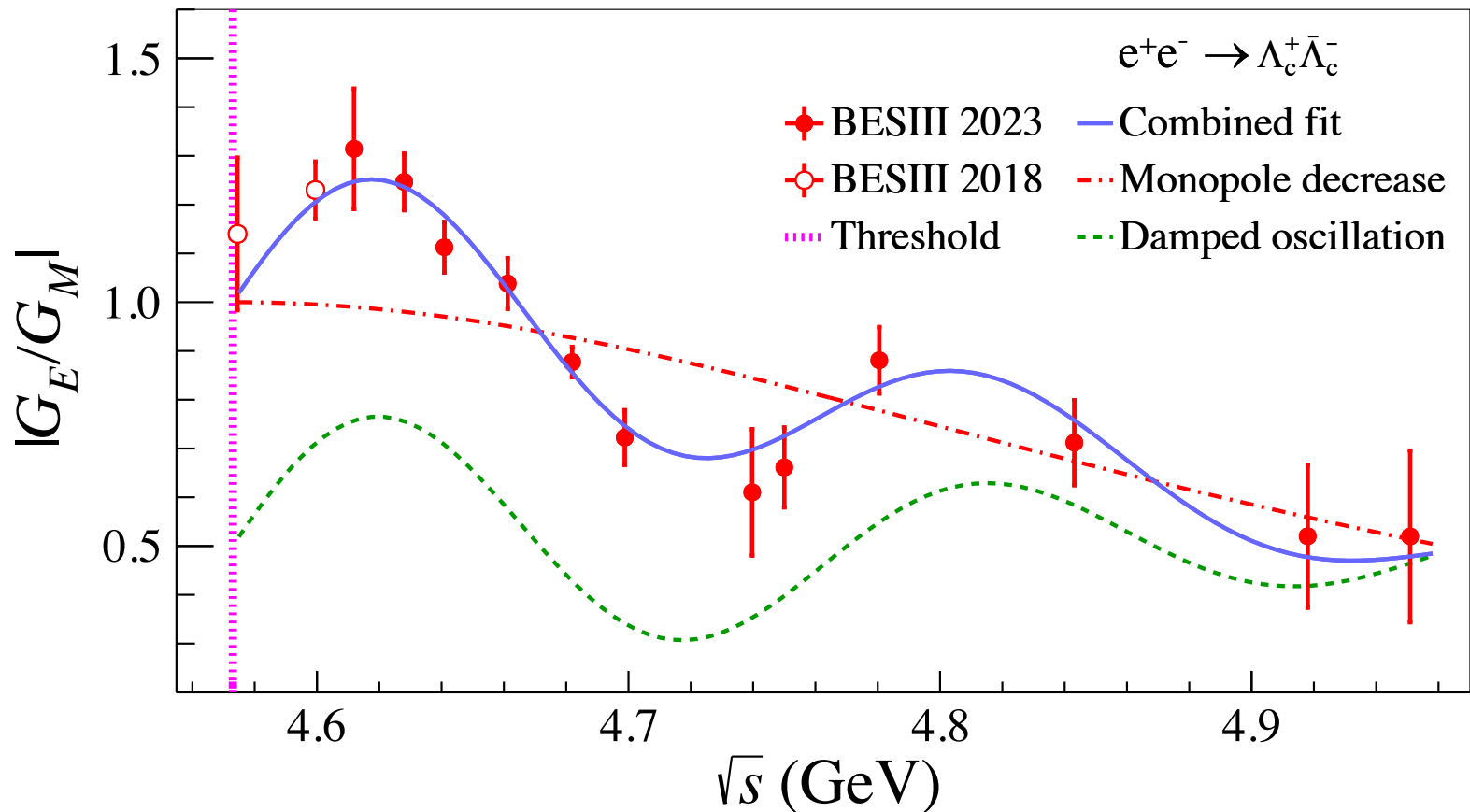
$$f(\cos\theta) \propto N_0 (1 + c_0 \cos\theta + \alpha_{\Lambda_c} \cos^2\theta)$$

E. Tomasi-Gustafsson et al., PRC 103, 035203 (2021)

where c_0 reflects the contribution from two-photon exchange process. **Vanishing c_0 is obtained at each c.m. energy, no contribution from TPE process**

- Cross feed between different $\cos\theta$ bins are considered via performing an unfolding based on the signal MC samples, **negligible effects to $|G_E/G_M|$**
- Different binning scheme in terms of $\cos\theta$ is tested, including 8, 12, 16, 26, 32, and 40, **no systematic deviation from the nominal case (20) is observed**
- Sufficient input-output checks are carried out based on larger-statistic signal MC samples, **the angular-analysis approach is valid**
- A plenty of systematic effects are considered, **the total uncertainty is dominated by the statistical one**

Electromagnetic form factor of Λ_c^+

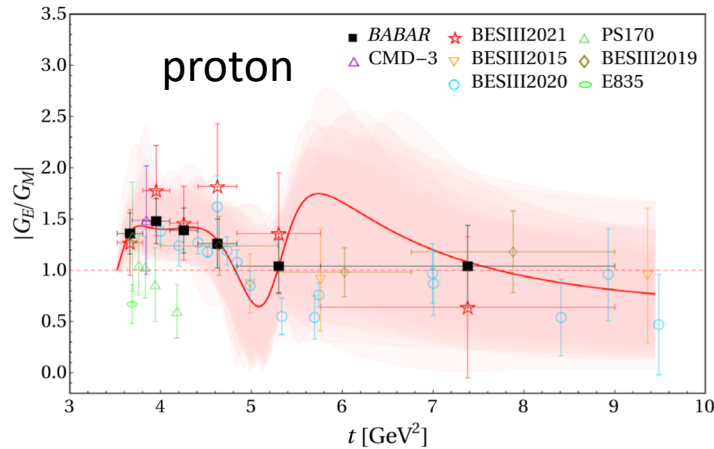
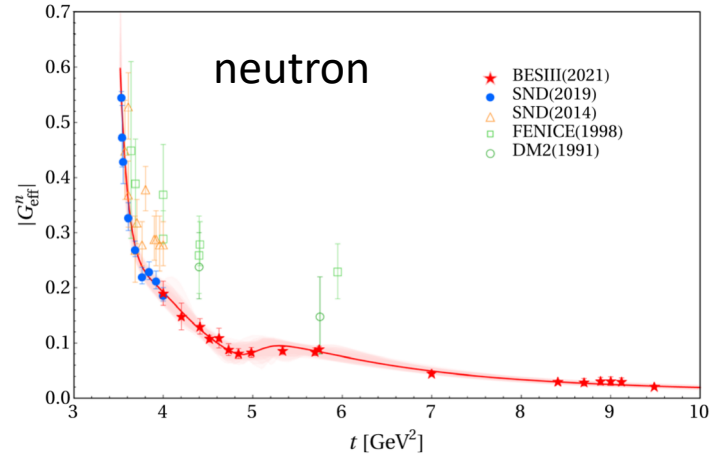
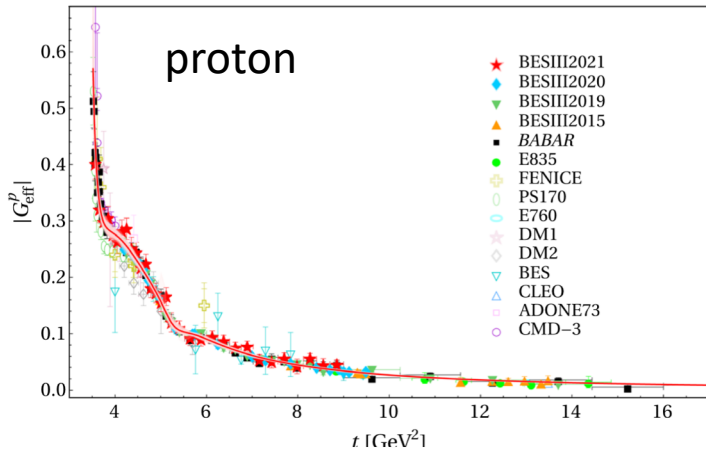


- Fitted to a function combining **monopole decrease** with **damped oscillation**
- **Oscillation feature** is unambiguously discerned for the charmed baryon Λ_c^+

Where is the oscillation from?

Dispersion theory: **broad poles above threshold in nucleon**

Yong-Hui Lin, Hans-Werner Hammer, and Ulf-G. Meißner, Phys. Rev. Lett. **128**, 052002 (2022)



V_s	M_V	Γ_V	a_1^V	a_2^V
ω	0.783	0	0.701	0.338
ϕ	1.019	0	-0.526	-0.997
s_1	1.031	0	0.422	-2.827
s_2	1.120	0	0.122	3.655
s_3	1.827	0	0.955	-1.122
r_{s1}	1.903	0.973	-2.653	-1.753
r_{s2}	1.914	0.541	-3.069	2.017
r_{s3}	1.879	0.895	4.953	0.501

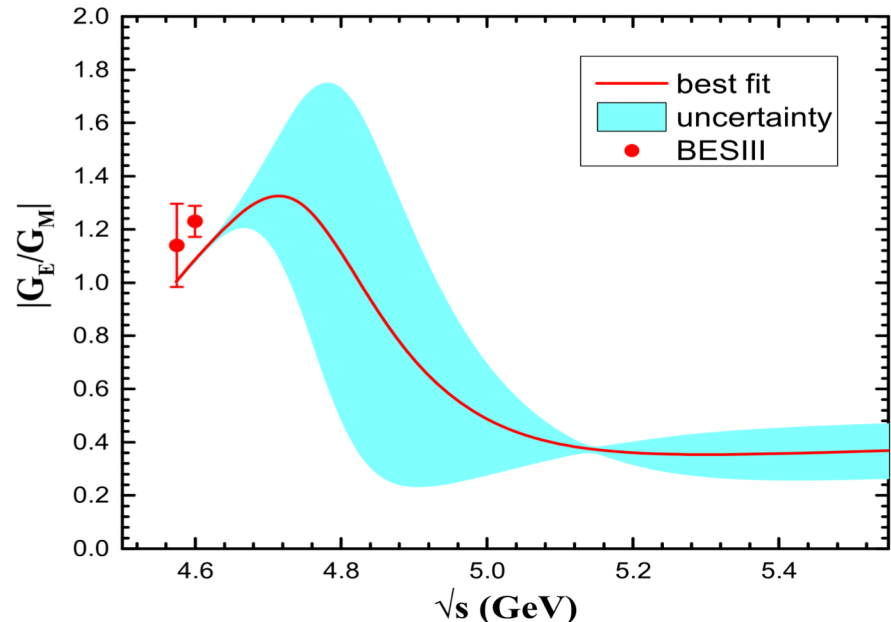
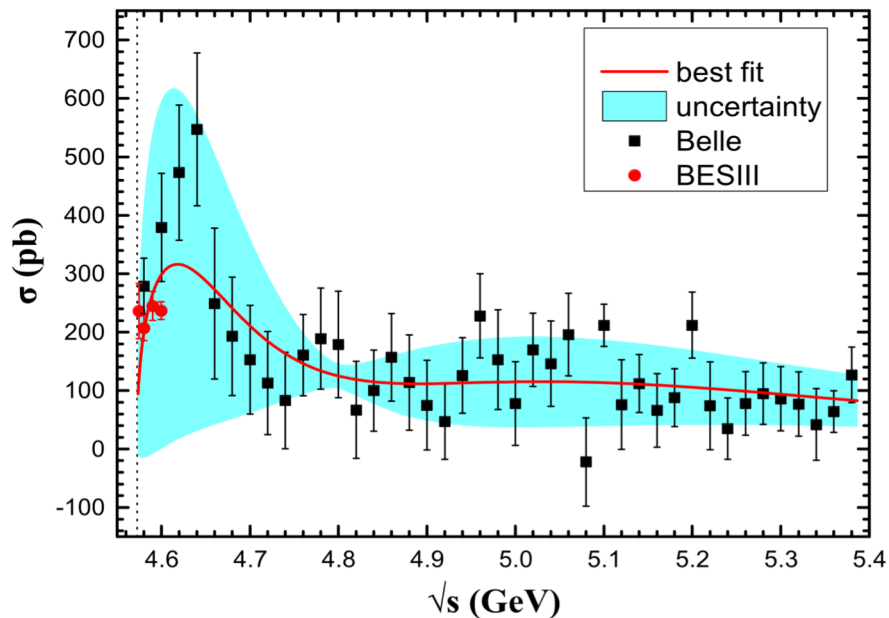
V_v	M_V	Γ_V	a_1^V	a_2^V
v_1	1.050	0	0.782	-0.132
v_2	1.323	0	-4.873	-0.645
v_3	1.368	0	3.518	-0.987
v_4	1.462	0	2.243	-3.813
v_5	1.532	0	-1.422	3.668
r_{v1}	2.256	0.239	2.552	-1.217
r_{v2}	2.253	0.245	-1.947	0.551
r_{v3}	2.220	0.362	-0.985	1.061

May not applicable for Λ_c^+ be since no oscillation feature is observed $|G_{\text{eff}}|$ data

Where is the oscillation from?

A prediction of $|G_E|$ and $|G_M|$ based on the **modified VMD model** :

Junyao Wan, Yongliang Yang, and Zhun Lu, Eur. Phys. J. Plus 136, 949 (2021).



- $|G_E|$ and $|G_M|$ are parameterized separately with the modified VMD model
- Contribution from the vector charmed mesons and their excitations are included
- Phenomenology parameters are determined by fitting BESIII and Belle cross section data and BESIII $|G_E/G_M|$ data

Maybe difficult to simultaneously reproduce new BESIII cross section and $|G_E/G_M|$ data

Summary and outlook

- BESIII measured the cross section and electromagnetic form factors of $e^+e^- \rightarrow \Lambda_c^+ \bar{\Lambda}_c^-$ with unprecedented precision
- The cross-section plateau is confirmed up to 4.66 GeV and the decay process $Y(4630) \rightarrow \Lambda_c^+ \bar{\Lambda}_c^-$ is not observed
- Contradict to the case in proton and neutron, the oscillation feature is not observed in the $|G_{\text{eff}}|$ spectrum of Λ_c^+
- Oscillation is discerned in $|G_E/G_M|$ distribution of Λ_c^+ , but with a significantly different frequency from that of proton

It is likely that these two oscillations come from different origins

Summary and outlook

- BESIII will collect data at energies up to 5.6 GeV, more charmed baryons, such as Λ_c^* , Σ_c , Ξ_c and Ω_c , could be studied

Chin. Phys. C 44, 04001 (2020)

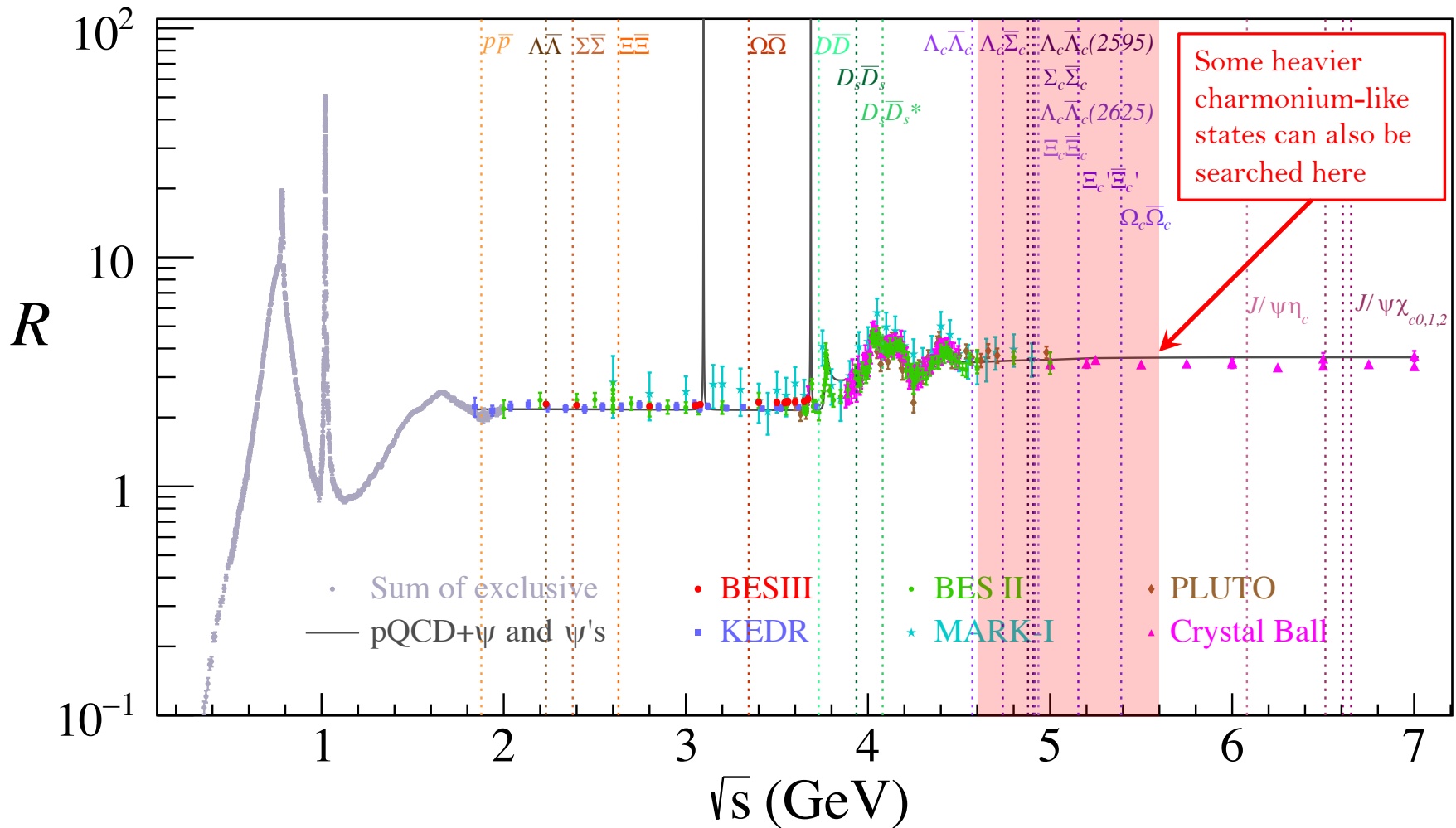
Table 7.1: List of data samples collected by BESIII/BEPCII up to 2019, and the proposed samples for the remainder of the physics program. The most right column shows the number of required data taking days in current (T_C) or upgraded (T_U) machine. The machine upgrades include top-up implementation and beam current increase.

Energy	Physics motivations	Current data	Expected final data	T_C / T_U
1.8 - 2.0 GeV	R values Nucleon cross-sections	N/A	0.1 fb ⁻¹ (fine scan)	60/50 days
2.0 - 3.1 GeV	R values Cross-sections	Fine scan (20 energy points)	Complete scan (additional points)	250/180 days
J/ψ peak	Light hadron & Glueball J/ψ decays	3.2 fb ⁻¹ (10 billion)	3.2 fb ⁻¹ (10 billion)	N/A
$\psi(3686)$ peak	Light hadron & Glueball Charmonium decays	0.67 fb ⁻¹ (0.45 billion)	4.5 fb ⁻¹ (3.0 billion)	150/90 days
$\psi(3770)$ peak	D^0/D^\pm decays	2.9 fb ⁻¹	20.0 fb ⁻¹	610/360 days
3.8 - 4.6 GeV	R values XYZ /Open charm	Fine scan (105 energy points)	No requirement	N/A
4.180 GeV	D_s decay XYZ /Open charm	3.2 fb ⁻¹	6 fb ⁻¹	140/50 days
4.0 - 4.6 GeV	XYZ /Open charm Higher charmonia cross-sections	16.0 fb ⁻¹ at different \sqrt{s}	36 fb ⁻¹ at different \sqrt{s}	770/310 days
4.6 - 4.9 GeV	Charmed baryon/ XYZ cross-sections	0.56 fb ⁻¹ at 4.6 GeV	15 fb ⁻¹ at different \sqrt{s}	1490/600 days
4.74 GeV	$\Sigma_c^+ \Lambda_c^-$ cross-section	N/A	1.0 fb ⁻¹	100/40 days
4.91 GeV	$\Sigma_c \Sigma_c$ cross-section	N/A	1.0 fb ⁻¹	120/50 days
4.95 GeV	Ξ_c decays	N/A	1.0 fb ⁻¹	130/50 days

A refined energy-scan will always help for the study of the $e^+e^- \rightarrow \Lambda_c^+ \bar{\Lambda}_c^-$ process!

Summary and outlook

- BESIII will collect data at energies up to 5.6 GeV, more charmed baryons, such as Λ_c^* , Σ_c , Ξ_c and Ω_c , could be studied



Summary and outlook

Thank you!

Summary and outlook

- BESIII will collect data at energies up to 5.6 GeV, more charmed baryons, such as Λ_c^* , Σ_c , Ξ_c and Ω_c , could be studied

